Marine oolites as proxies for palaeoenvironmental reconstructions during extinction events.

Urban, Ingrid

2023

LITHOLUND THESES 39

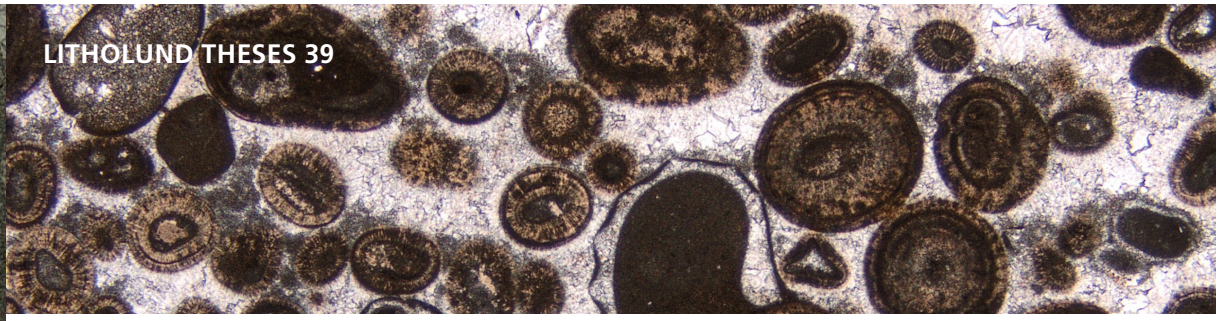

Marine oolites as proxies for palaeoenvironmental reconstructions during extinction events

INGRID URBAN
LITHOSPHERE AND BIOSPHERE SCIENCE | DEPARTMENT OF GEOLOGY | LUND UNIVERSITY 2023

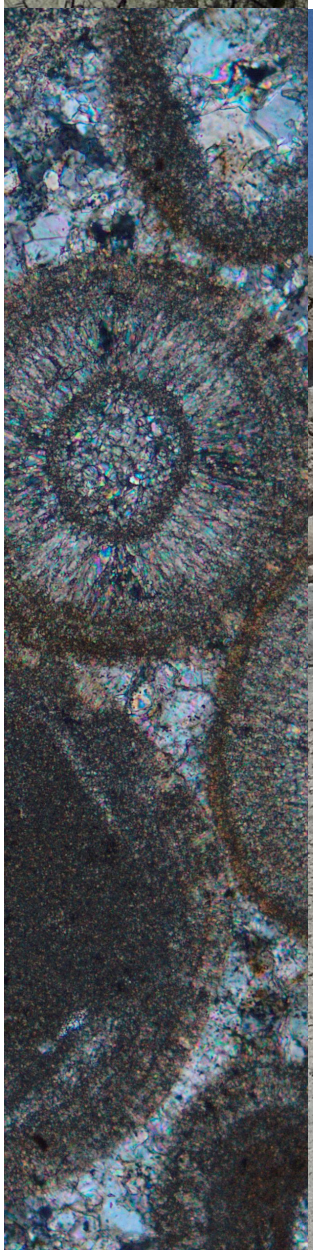

Printed by Media-Tryck, Lund 2023 NORDIC SWAN ECOLABEL 3041 0903

Panoramic view from Pufels/Bulla outcrop

LUND UNIVERSITY

Lithosphere and Biosphere Science
Department of Geology
Lund University
Sölvegatan 12
SE-223 62 Lund, Sweden
Telephone +46 46 222 78 80

ISSN 1651-6648
ISBN 978-91-87847-76-9

LITHOLUND THESES 39

Marine oolites as proxies for palaeoenvironmental reconstructions during extinction events

Ingrid Urban

LUND
UNIVERSITY

Lithosphere and Biosphere Science
Department of Geology

DOCTORAL DISSERTATION
by due permission of the Faculty of Science, Lund University, Sweden.
To be defended at Department of Geology, Sölvegatan 12, 22362 Lund on the 12th of May at 13:15.

Faculty opponent
Professor Rachel Wood
University of Edinburgh

Cover picture: Ingrid Urban

Lithosphere and Biosphere Science
Department of Geology
Faculty of Science

ISBN 978-91-87847-76-9 (print)

ISBN 978-91-978-91-87847-77-6 (pdf)

Organization

LUND UNIVERSITY
Department of Geology
Sölvegatan 12
SE-223 62 Lund
Sweden

Author: Ingrid Urban

Document name

DOCTORAL DISSERTATION

Date of issue: 12th of May 2023

Sponsoring organization

Marine oolites as proxies for palaeoenvironmental reconstructions during extinctions events

Abstract

At present time, it has been stated that "Human activities, principally through emissions of greenhouse gases, have unequivocally caused global warming, with global surface temperature reaching 1.1°C above 1850–1900 in 2011–2020". Therefore, understanding the consequences of human activities on present and future climate is one of the most important issues of this century. It is not the first time that extreme climate conditions are recorded in the Earth geologic record. Sometimes they affected the whole planet so deeply that they led to vast biodiversity breakdowns both in the oceans and on the continents, causing the disappearance of most living species. That is the case of mass extinction events. Looking for reliable proxies to better reconstruct climate conditions during extreme past events could help to predict climate evolution in high-stressed conditions, such as the one of the last decades. The present dissertation aims at digging into the broad field of palaeoenvironmental reconstruction using a potentially successful proxy: marine ooids and their lithified equivalent, oolites. Ooids are tiny (less than 2 mm) carbonatic marbles made of exceptionally thin, concentric layers around a nucleus. They accumulated in anomalously thick deposits after major biodiversity crises. The scope of this dissertation is to recover specific chemical and physical conditions of the ocean water after two mass extinction events, the end-Permian and the end-Triassic. For the former, I described ooids from the Italian Dolomites and for the latter from the United Arab Emirates, using several advanced analytical techniques. By using optical and scanning electron microscopy, I carefully described their internal structure and monitored how different types and sizes of ooids co-varied in time in the immediate aftermath of the extinction events. I also obtained chemical information from the ooids and other components of the rock samples by using elemental mapping techniques with scanning electron microscopy and laser ablation coupled to mass spectrometry. In order to widen our perspective on the environmental consequences of extinction events, I also describe a thick sedimentary section in Wadi Milaha (UAE) and analyze its $\delta^{13}C_{carb}$ and $\delta^{18}O_{carb}$ isotopic record. I could demonstrate an original deposition in calcite of this oolite in contradiction with the accepted hypothesis and give an explanation for this. I could show as well that the formation of ooids after the end-Triassic Mass Extinction was favored by the income of water rich in phosphate on shallow environments. The end-Permian ooids could show the impact of the diagenesis on these proxies and which chemical elements are preserved and which are not. The palaeoenvironmental data I provided add new information on how the oceans reacted to extreme events in the past.

Key words Ooids; Permian-Triassic Boundary, Triassic-Jurassic Boundary; Arabian Platform; Southern Alps; palaeoenvironmental reconstruction

Classification system and/or index terms (if any)

Supplementary bibliographical information | Language

ISSN and key title: 1651-6648 LITHOLUND THESES | ISBN 978-91-87847-77-6

Recipient's notes | Number of pages 119 | Price

Security classification

Signature: Date: 27/03/2023

Contents

List of papers

This thesis is based on the three papers mentioned below, which are attached to the thesis. Paper I is reprinted under permission of Elsevier.

Paper I
Urban, I., Demangel, I., Krystyn, L., Calner, M., Kovács, Z., Gradwohl, G., Lernpeiss, S., Maurer, F., and Richoz, S. (2023). Mid-Norian to Hettangian record and time-specific oolites during the end-Triassic Mass Extinction at Wadi Milaha, Musandam Peninsula, United Arab Emirates. Journal of Asian Earth Sciences: X, 9, 100138. https://doi.org/10.1016/j.jaesx.2023.100138

Paper II
Urban, I., Richoz, S., Calner, M., Scherstén, A., and Naeraa, T. (2023). Insights on the Aragonite Sea II-Calcite Sea II transition through geochemical characterization of post-End-Triassic Mass Extinction ooids at Wadi Milaha, Musandam Peninsula, United Arab Emirates. Manuscript.

Paper III
Urban, I., Richoz, S., Calner, M., Scherstén, A., Naeraa, T., and Demangel, I. (2023). Geochemical characterization of post-end-Permian Mass Extinction ooids in the Italian Dolomites. Manuscript.

Acknowledgements

I started my PhD project five years ago, with lots of expectations but few certainties. It has been a long journey, where light and darkness chased each other for a long time. In the end, I can say that light prevailed and it is a good reason to be even more thankful, to both people and Life.

Let me start with my main supervisor Sylvain, who has welcomed me since day one with open arms. It is not easy to summarize all the good and bad adventures we have had, but I am incredibly proud to have finished this PhD project without giving up. I would also like to thank my other supervisors Mikael and Anders. You have always been helpful and your input has been invaluable. Then, a special thought to Isaline and Zsófi. Isaline, it was a pleasure working with you. You have always given me great support with a smile. We also shared some good times outside of work, I always enjoyed them. Zsófi, it was so nice to have you as part of the team and to share the memories of our time as PhD students. I am also grateful to my other co-authors, they always gave me good ideas to improve the manuscripts. A special mention goes to Tomas and his technical support. I would like to thank Johan Lindgren and Helena Filipsson for their help through all PhD requirements and deadlines.

In summer schools and conferences around the world, I met so many enthusiastic researchers. There I had the opportunity to share inspiring conversations about carbonates and mass extinctions. A special mention goes to the Carbonate Crew.

Among the people who first welcomed me here in Lund, I cannot forget Ashley and Anders Lindskog, who respectively provided my first accomodation and patiently taught me the secrets of thin sections preparation.Thank You guys, you were always so kind to me!

Among the administrative and technical personnel at the department, a special thank you goes to Gert, Britta, Åsa, Git and all present and past staff at Kansli.

I shared nice conversations with so many people here at the department, I always felt welcome to join and share my thoughts.

And now it's time for the people who are my point of reference in Sweden: all PhD students and postdocs at the Department of Geology! I had the opportunity to meet so many beautiful people, who are not just colleagues but friends. Some of them have left Sweden, others are still here and I have good memories of all of them. Among them, I would like to thank once again Martin, Rosine, Sofia, Guillaume, Sha, Carla and Markus, Bingjie, Petra, Florian, Chiara, Franzi, Anna, Marie, Tjördis, Kristin, Constance and Gabriel. Another special thought is for my office mates (Maria, Cindy, Karola, Josefin and Miguel). I never felt alone in the big office, your presence and support have been fundamental.

A final mention goes to the undergraduate students with whom I shared my love for carbonates, especially Johannes and Linus.

I cannot conclude without introducing the people who support me from Italy: my family and friends. Grazie per avermi tenuta sempre con voi, per l'affetto e la comprensione. Voglio nominare alcuni di voi in particolare, perché avete fatto davvero la differenza: Giacomo, Eleonora, Alberto, Linda, Mirko, Alessandro, Angelo, Nicola, Lucrezia, Michele, Yasmin e il mio caro Juri. Da ultimo, proprio perché imprescindibile, dedico il pensiero più dolce ai miei genitori e alla mia nonna Maria: mi avete insegnato molto della vita, siete e sarete sempre la mia roccia.

Abbreviations

Below we list the most common abbreviations used in this thesis.

EPME: end-Permian Mass Extinction

ETME: end-Triassic Mass Extinction

PTB: Permian-Triassic Boundary

BWB: Bellerophon-Werfen formational boundary

TJB: Triassic-Jurassic Boundary

SEM (or FE-SEM): Scanning Electron Microscopy (or Field Emission-Scanning Electron Microscopy)

EDS: Energy Dispersive X-ray Spectroscopy

EBSD: Electron Backscatter Diffraction

LA-ICP-MS: Laser Ablation-Inductively Coupled Plasma-Mass Spectrometry

EPS: Extracellular Polymeric Substance

ACC: Amorphous Calcium Carbonate

Introduction

At present time, it has been stated that "Human activities, principally through emissions of greenhouse gases, have unequivocally caused global warming, with global surface temperature reaching 1.1°C above 1850–1900 in 2011–2020" (IPCC, 2023). Therefore, understanding the consequences of human activities on present and future climate is one of the most important issues of this century. It is not the first time that extreme climate conditions are recorded in the Earth geologic record. Sometimes they affected the whole planet so deeply that they led to vast biodiversity breakdowns both in the oceans and on the continents, causing the disappearance of most living species. That is the case of mass extinction events. Looking for reliable proxies to better reconstruct climate conditions during extreme past events could help to predict climate evolution in high-stressed conditions, such as the one of the last decades (Benton, 1995). The present dissertation aims at digging into the broad field of paleoenvironmental reconstruction using a potentially successful proxy: marine ooids and their lithified equivalent, oolites. In the field of carbonate sedimentology, these coated grains have always been considered an interesting object of study. Already in the 19th century, they were recognized and carefully described (Lyell 1855, Sorby 1879). Although efforts were put to understand their morphology and formation mechanism, it was only since the last decades that researchers focused on their geochemical significance and potentials. Like tree rings, their concentric layers accrete on a yearly or decadal time interval. A single grain may form in about 800 years (Beaupré et al., 2015) and register physicochemical variations occurring in their ambient environment (i.e., marine or terrestrial). Their geochemical signature, if original, gives them the potentiality to constitute an archive for paleoenvironmental conditions. This dissertation focuses on marine carbonate ooids that deposited immediately after two mass extinction events (end-Permian and end-Triassic). Ooid deposition is considered anomalously if abundant and widespread, although they are found in most time periods from the Late Archean (Sumner & Grotzinger 1993) to the present (Simone 1980). For the end-Permian Mass Extinction (EPME), we sampled four end-Permian-Triassic sections in the Italian Dolomites. For the end-Triassic Mass Extinction (ETME),we sampled a mid-Norian-Hettangian section in the Musandam Peninsula (United Arab Emirates) and two shorter coeval sections that span through the ETME interval. The analytical approach is morphological and geochemical. Optical microscopy and scanning electron microscopy (SEM) gave insights into morphological features of the ooids structure at mm and μm scale, while in situ mass-spectrometry (LA-ICP-MS) provided geochemical data on ooids composition, together with elemental mapping (EDS and EBSD). Besides, bulk isotopic analyses for $\delta^{13}C_{carb}$ and $\delta^{18}O_{carb}$ were performed on different components of post-ETME oolitic samples (coated grains, matrix, and cement), to be compared with the general mid-Norian-Hettangian isotopic record.

Scope of the thesis

The main aim of this dissertation is to better assess the potential of ooids for untangling the palaeoceanographic conditions during periods of profound biotic and environmental turnovers. To be able to reach this aim I had several objectives:

1. Provide a detailed morphological description of post-EPME and post-ETME ooids from key stratigraphic sections.

2. Investigate the primary mineralogy of post-EPME and post-ETME ooids, to implement in the global record of "Aragonite Sea-Calcite Sea" alternation.

3. Distinguish as far as possible the original seawater geochemical signal in the ooids from diagenetic alteration.

4. Interpret the obtained geochemical signal in terms of depositional settings.

5. Once the geochemical signal in the ooids has been separated from interferences due to diagenesis and local depositional conditions, try to interpret it in terms of seawater conditions in the aftermath of the EPME and ETME events.

In addition to the above-mentioned objectives, in this work I described the sedimentology, stratigraphy, and the δ13Ccarb and δ18Ocarb isotopic records of Wadi Milaha, a key section for the mid-Norian through Hettangian paleoenvironmental evolution in low latitudes. It gives a unique insight into the environmental crises at the Norian-Rhaethian Boundary and during the ETME.

Background

Oolites and ooids

Oolites are the lithified equivalent of ooids. An ooid is a spherical or sub-spherical coated grain made of a nucleus surrounded by concentric layers, which form a laminated cortex. By definition, ooids diameter is less than 2 mm (Carozzi, 1960). According to this author, this threshold is a product of hydrodynamics and abrasion processes. A grain bigger than 2 mm would not be able to stay suspended in water for any prolonged time and this would stop or significantly slow down its growth. Increasing abrasion would also contribute to limit the size. However, there are exceptions to this definition, like the case of giant ooids described in Li et al. (2013) and Tan et al. (2018). The cortex can be made of carbonate or other minerals, for instance iron, silica or phosphates (Flügel, 2010). Ooids are classified as radial, tangential or micritic, according to the arrangement of the crystals in the cortex laminae (Fig. 1) (Flügel, 2010). Ooids can be found as single or compound (Flügel, 2010). Among compound ones are "polyooids", which are grains whose nucleus is made of two or more complete ooids bound together (Flügel, 2012). Ooids are called "superficial" when their cortex is less than half of the whole diameter (Flügel, 2010). Both modern and ancient ooids can nucleate in marine or non-marine environments. They are considered important proxies for palaeoclimatic and palaeoceanographic reconstruction, e.g., to determine water energy levels, water depths, salinity, sedimentary environment, climate conditions, as well as seawater chemistry (Bathurst, 1972; Simone, 1980; Peryt, 1983; Sandberg, 1983; Tucker et al., 1990; Hardie, 2003; Siewers, 2003; Flügel, 2010).

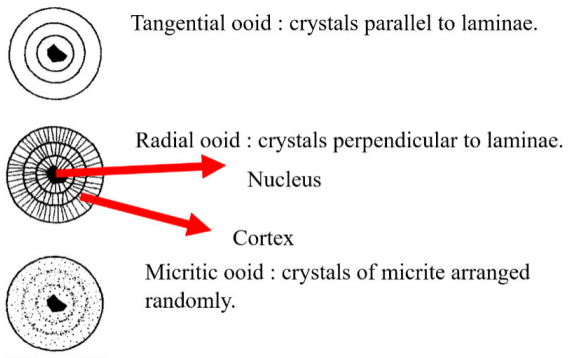

Fig. 1 Classical morphological classification of ooids (Flügel, 2010).

Formation environments

According to Flügel (2010) modern marine ooids are found in intertidal and shallow subtidal marine environments, restricted to the tropical warm pools (Li et al., 2019); non-marine ooids form in lacustrine and terrestrial settings instead. Ooids can be "high-energy ooids" or "quiet water ooids", both forming along ooid shoals (Diaz et al., 2014). Ooid sand shoals, like those of Bahamas Archipelago, represent marine sand belts and tidal bar belts parallel to a carbonate platform margin or platform interior blankets. Ooid shoals are subdivided in three different environments. In the shoal crest, high hydrodynamic energy sorts the sediments, which are composed of 90% ooids (active shoal). In the flank of the shoal, hydrodynamic energy diminishes, as well as sorting and ooids content in the sediment (60-80%, non-active shoal). Instead, in topographical lows located on the shoal crest or tidal flat, the energy regime is extremely low and microbial biofilm or cyanobacteria coating interact with ooids (microbially stabilized zones). In addition, quiet water ooids are also common in lagoons, coastal lakes and other terrestrial or marine shallow environments not swept by strong waves but with strong changes in salinity (Flügel, 2010). A quiet water ooid is usually less spherical than a high-energy one, due to minor wind and waves' action. Radial ooids form normally in low-energy conditions, while tangential ooids deposit in high-energy conditions (Flügel, 2010). The same kind of depositional setting is extended to ancient ooids, with some specific exceptions. For instance, iron ooids were particularly abundant in Ordovician-Devonian and Jurassic-Early Paleogene in lagoonal and back-bar environments, as in deeper marine environments just above the storm-wave base (Utescher, 1992; Gygi, 1981). However, this example does not contradict the fact that the majority of ooids found in deep water are allochthonous shallow-water material transported as debris flows or turbidites (Flügel, 2010).

Ooids origin: organic vs. inorganic

Marine ooids have different mineral composition, such as calcium carbonate (low-Mg and high-Mg calcite and aragonite), iron, silica and phosphate. They usually form along the margins of carbonate platforms under specific physicochemical conditions and requirements (according to Duguid et al., 2010 these are): 1) Presence of a potential nucleus (a mineral crystal, a fossil fragment, a fecal pellet, a rock fragment); 2) Supersaturated water with respect to $CaCO_3$; 3) An agitated environment allowing frequent refreshing and degassing of CO_2. Even if the physicochemical model has been the leading one for decades, evidence of biological influences in this process has been mentioned by several studies. Davies et al. (1978) already stressed the role of biofilms in favouring cortex formation in carbonate ooids, directly or indirectly. Indeed, these organisms can promote $CaCO_3$ precipitation in different ways. According to Dupraz et al. (2009), they can directly control precipitation through their cellular activities (biologically-controlled mineralization) or setting favourable pH and alkalinity conditions for crystal nucleation through their metabolic processes (biologically-induced mineralization); organic matrix, such as EPS (Extracellular Polymeric Substance), can also act as a substrate for crystal nucleation (biologically-influenced mineralization). Several studies, both on fossil and recent ooids, investigated different aspects of biologically-influenced or biologically-induced mineralization in ooids. For example, in Quaternary Bahamas oolitic sands, Diaz et al. (2014) traced all different functional genes in microbial communities that identify metabolic processes for carbonate precipitation; a consortium of oxigenic/anoxic photoautotrophs, oxygenic/anoxic heterotrophs, denitrifiers, sulfate reducers and ammonifiers mainly forms such communities. The authors also detected genes related to EPS-degrading enzymes (i.e., chitinases, glucoamylase, amylases), proving the presence of altered EPS in oolitic sands. Altered EPS releases Ca^{2+} cations from its matrix and creates accretion spots for $CaCO_3$ (Dupraz & Visscher, 2005; Baumgartner et al., 2006). Diaz et al. (2017) analysed the same ooids from Bahamas and stressed the role of altered EPS and different living organisms (filamentous fungi, cyanobacteria, biofilm-forming diatoms) in promoting the precipitation of ACC (amorphous calcium carbonate). ACC was proved the fundamental metastable precursor to aragonite nucleation in ooids laminae (Diaz et al., 2017). Some evidence of similar interaction between ooids and bacteria during the formation stage has been provided also from past oceans. For instance, Li et al. (2017) investigated Lower Triassic marine ooids from South China and traced microbial filaments- and EPS- like structures; higher content in REE and nutrient-like elements as Ba characterize the laminae where these structures were found. These ooids formation has

been thus explained as a product of organomineralization by photosynthetic organisms. In specific cases, physicochemical conditions are almost irrelevant in shaping ooids, as in the case of modern freshwater ooids in Lake Geneva (Plee et al., 2008; Aritzegui et al., 2012). Despite the provided evidence, a biotic origin for ooids is still debated and other authors considered ooids only as a product of chemical and physical processes (e.g., Sumner & Grotzinger, 1993; Rankey & Reeder, 2009; Duguid et al., 2010; Trower et al., 2018).

Formation models

The accretion process in ooids follows a complex process, which has been reproduced through different models. Davies et al. (1978) proposed a model for ooids growing in an agitated environment in laboratory conditions, in which each period of active accretion was followed by resting and sleeping stages (Fig. 2). For larger grains, the precipitation of fringing cement in the ooids cortex was suggested to occur within dune sediment (Anderson et al., 2020). Diaz et al. (2017) implemented this model relative to the possible biotic origin of ooids (Fig. 3). They considered recent Bahamian ooids growing on an active shoal. During the so-called sleeping stage, EPS can attach to the outer surface of the ooid and become a substrate for ACC nucleation. Actual ACC nucleation and transformation into aragonite occurs during the resting stage, when ooids lay in the shallow subsurface or in low-energy portions of the shoal. After ooids are exposed to currents, the outer layers are polished and aragonite needles are arranged tangentially. When ooids are not exposed to high-energy, growth mechanism stops and post-formation micritization starts. More recently, Batchelor et al. (2018) published a third model (Fig. 4). They used a mathematical approach based on the way avascular brain tumors propagate in the human body. In a similar way as reasoned by Diaz et al. (2017), a biofilm colonizes a spherical surface and is characterized by two regions: an outer layer supplied by nutrients and an inner zone, where nutrients cannot diffuse. In the inner zone, organomineralization occurs and the ooid growth is radially symmetric and strictly dependent on the nutrient flux rate. In this way, the inner part does not grow biofilm anymore beyond a threshold size. "Suspension" and "resting" growth phases by Davies et al. (1978) are thus replaced by an alternation of mineralization driven by biofilm and following syngenetic mineral growth, in which organic matter and impurities do not become part of the growing crystal and instead are confined to the outer portion of the ooid. This model attributes the size of a hypothetical ooid more to nutrient and biomass supply than to physical parameter (i.e., water energy).Ooids size is limited as well, but the 2 mm threshold for ooids diameter is not considered.

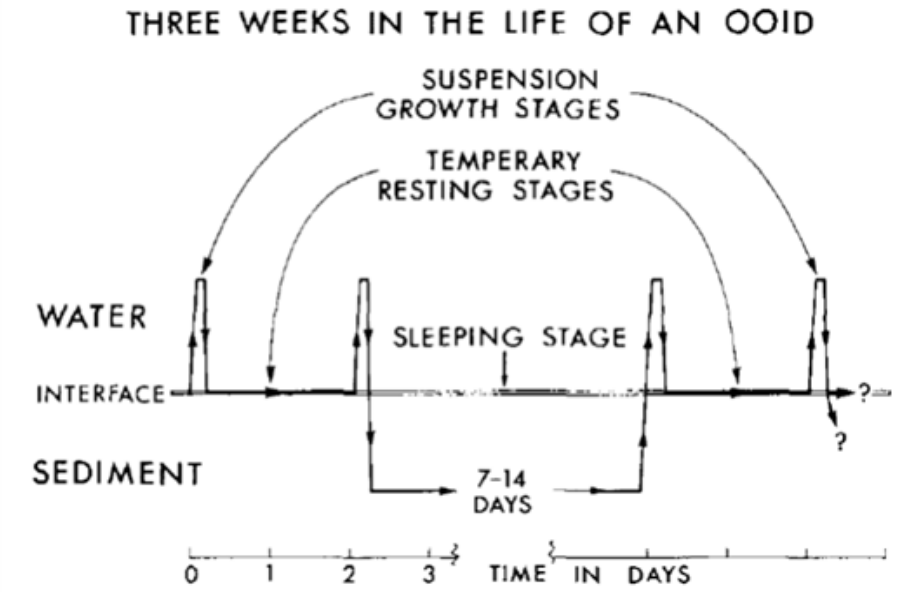

Fig. 2: Formation model for ooids in laboratory, under agitated conditions (Davies et al., 1978).

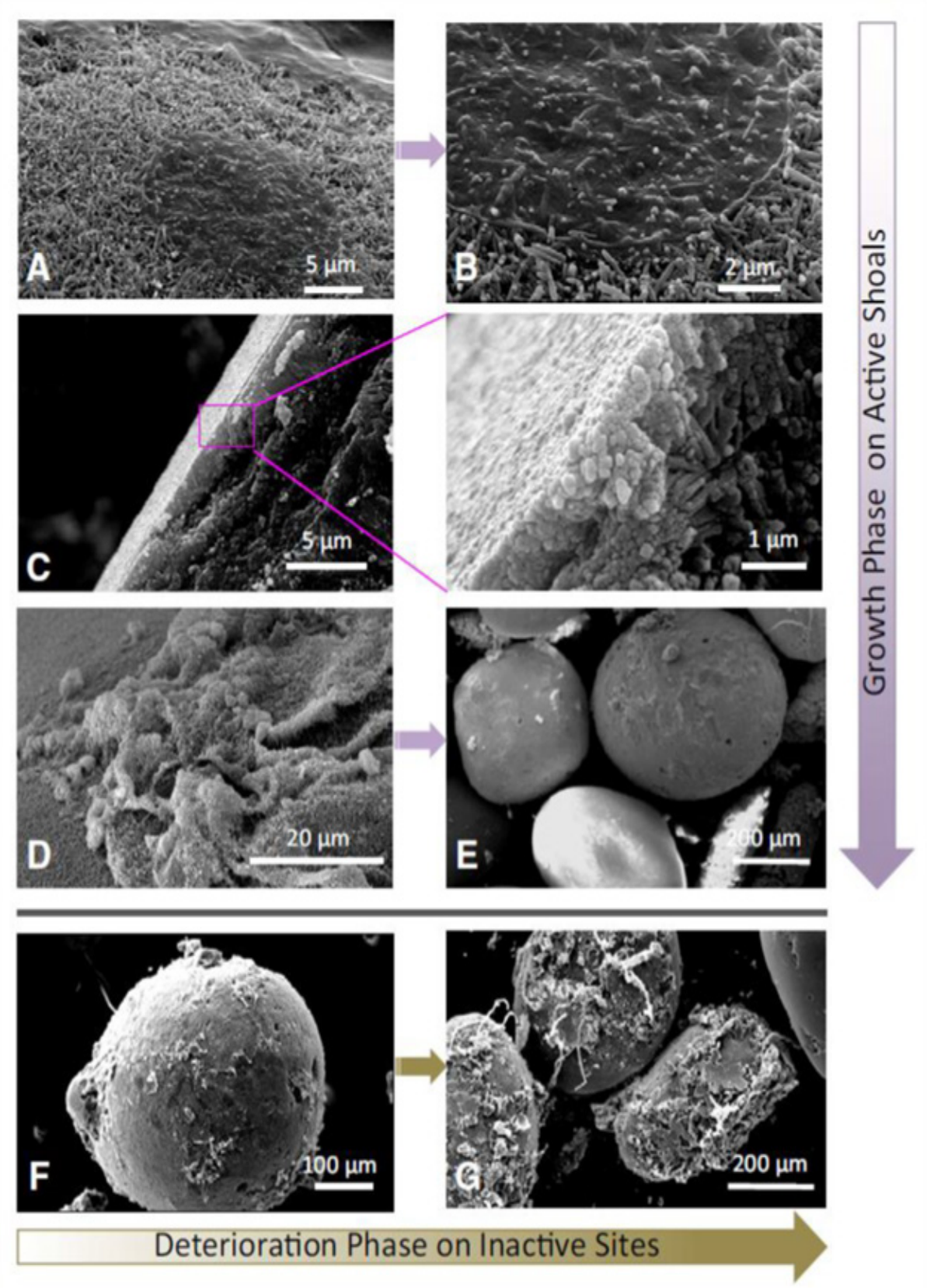

Fig. 3: Ooids formation model. A-B: precipitation of ACC mediated by EPS, C-D: thin layer of ACC forming; D: ACC replaced by aragonite crystals; E: polished surface on the ooid outer layer, made by turbulent water; F-G: microbes in the micritization stage (Diaz et al., 2017).

Fig. 4: ooids growth model described by Batchelor et al., 2018. In the first two steps, a biofilm is fed by nutrient, while in the following two steps the outer part of the ooid gets all the nutrients. In the last step, microbes living in the outer part of the ooid die and mineralization phase starts (Batchelor et al., 2018).

"Aragonite Sea-Calcite Sea" cyclicity in the Phanerozoic

In the Phanerozoic oceans, the primary mineralogy of non-skeletal components and marine cements and oolites have oscillated globally between aragonite ± high-Mg calcite (Aragonite seas) and low-Mg calcite (Calcite seas), on a 100-200 m.y. scale (Sandberg 1983; Stanley & Hardie 1999) (Fig. 5). The chemical threshold between high-Mg calcite and low-Mg calcite is set at 4 mol% $MgCO_3$. The alternation of Calcite and Aragonite seas follows a first-order cyclicity. Sandberg (1983) established two Calcite seas (Cambrian-late Mississippian; late Triassic or early Jurassic to early or mid-Cenozoic), where the precipitation of aragonite was inhibited, which alternate with three Aragonite seas (late Precambrian-early Cambrian, late Mississippian to late Triassic or early Jurassic; early or mid-Cenozoic to the present), where aragonite precipitation was facilitated. The record of Sandberg (1983), based on marine ooids and cements, was later implemented in datasets on non-skeletal carbonates, KCl/$MgSO_4$ evaporites, reef builders and sediment-producing algae by Hardie (1996) and Stanley & Hardie (1999). According to Sandberg (1983), the end-Permian and the early Triassic are comprised in the Aragonite II Sea. In more recent works (i.e., Li et al., 2015), the primary mineralogy of Early Triassic ooids as aragonitic is questioned, together with the stable geochemical composition of the ocean where they precipitated (Li et al., 2013). Similar uncertainties are reported for some transitions such as the Aragonite I/ Calcite I seas boundary (Cambrian-Ordovician) and the Aragonite II/Calcite II seas boundary (Late Triassic or Early Jurassic), as reported by Stanley & Hardie (1998).

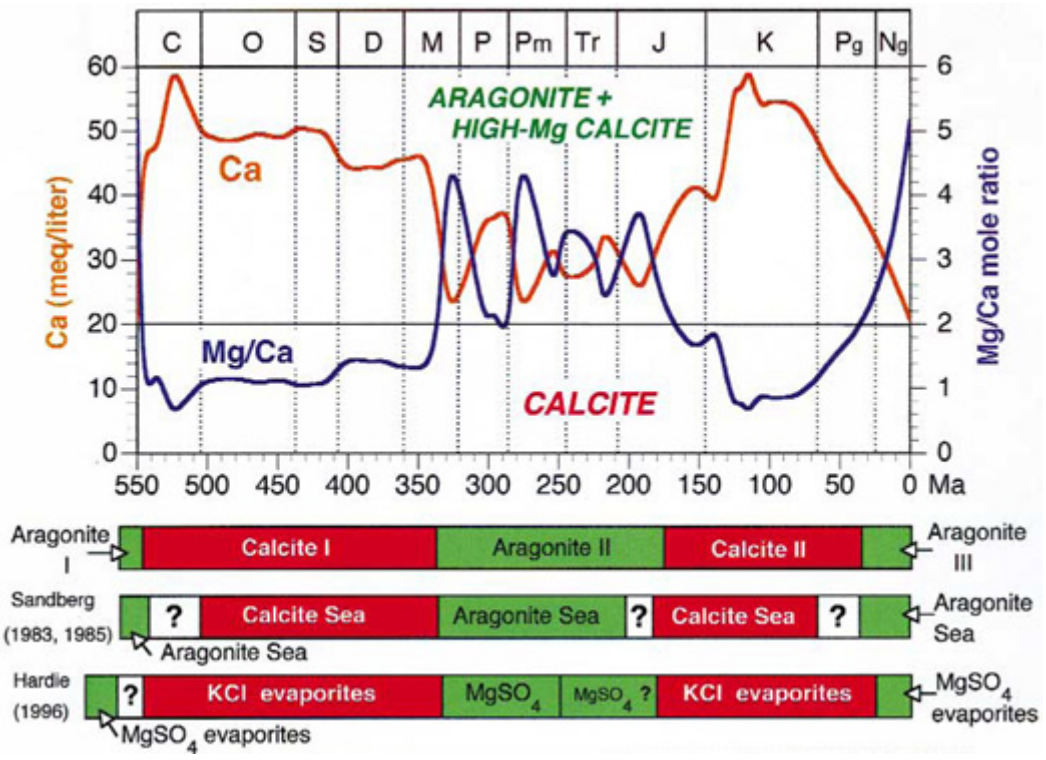

Fig. 5: Correspondence between secular oscillations for the carbonate mineralogy of dominant hypercalcifying marine taxa, the mineralogy of marine evaporites and nonskeletal carbonates, and the Mg/Ca ratio and absolute concentration of calcium (Ca) in seawater as calculated by Hardie (1996). A horizontal line at Mg/Ca = 2 (after Stanley and Hardie, 1998) defines the threshold of 4 mol% $MgCO_3$.

Mass extinction events

Earth history recorded a significant increase in Life diversity in seas and in the continents since the end of the Precambrian (Benton, 1995; Alroy et al., 2008). The fossil record also registers several biodiversity crises and extinction events, which provoked the disappearance of living families to different extents. Among all extinction events, Benton (1995) identified several major extinction events: Early Cambrian, Late Ordovician (Hirnantian, Katian), middle and late Devonian (Givetian, Frasnian, Famennian), Late Carboniferous (Moscovian, Gzelian), Late Permian (Changhsingian), end-Triassic (Rhaetian), end-Jurassic (Tithonian), mid-Cretaceous (Albian), end-Cretaceous (Campanian, Maastrichtian) and Late Eocene (Priabonian). Five of them show particularly high extinction percentages (Fig. 6) and occurred in Late Ordovician, Late Devonian, end-Permian, end-Triassic and end-Cretaceous. They are traditionally called "the Big Five" to highlight their deep and sudden impact on many biotic groups on a global scale. Among them, the end-Permian one was already considered the most severe extinction event of the Phanerozoic by Sepkoski (1982). Different methods have been applied to measure the effect of mass extinctions on biodiversity, such as the number of extinct families, percentage of extinction, total and per-family extinction rates (Benton, 1995). These approaches can overestimate or underestimate the real extinction impact, in relation to the chosen time unit or the relative diversity range for a certain time interval. Several hypotheses have been proposed on the actual causes of mass extinction events (for example meteorite impacts, emplacement of Large Igneous Provinces (LIPs), dramatic changes in global sea level and global changes in oceanic and atmosphere chemistry), but the idea of a periodicity due to a common and repetitive cause was refused (Benton, 1995).

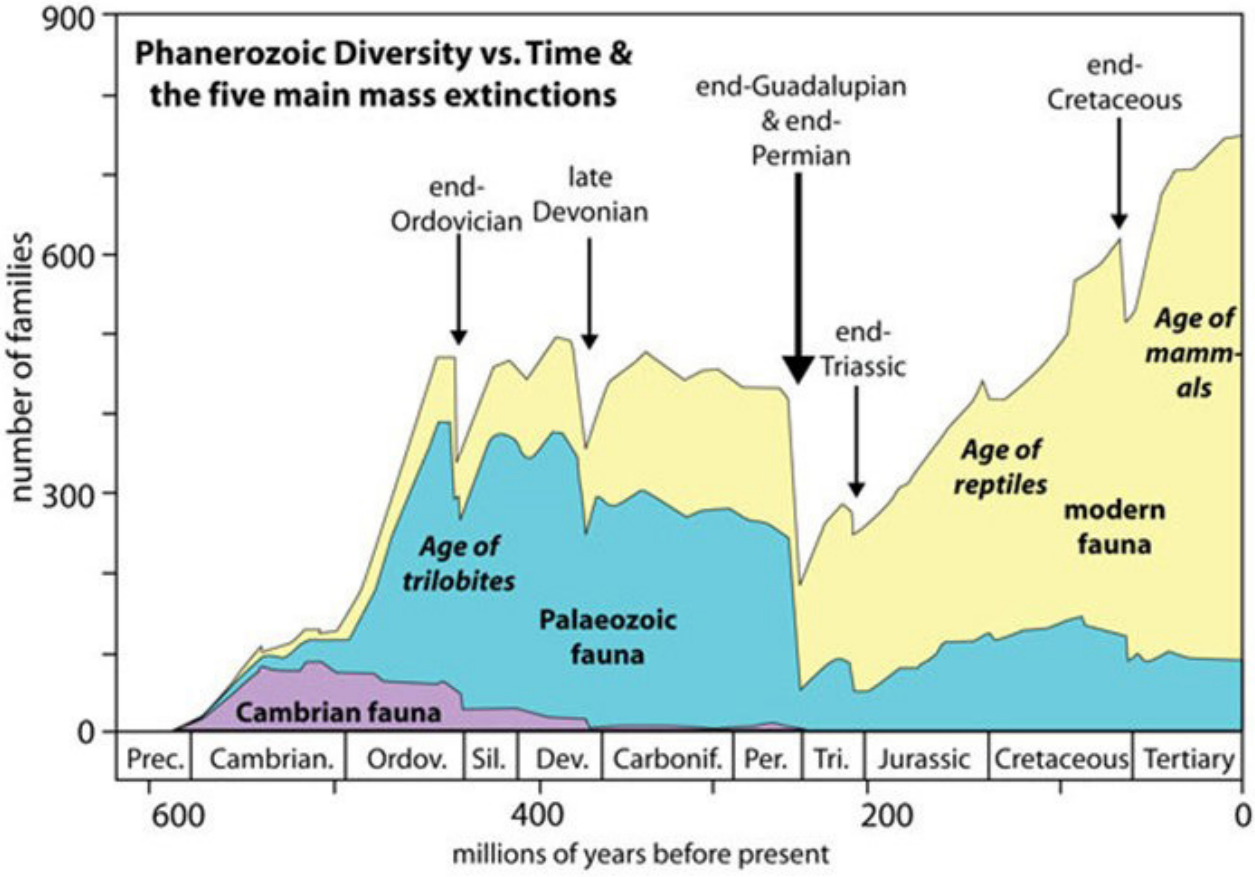

Fig. 6: Number of families during the Phanerozoic, with time position of the five mass extinction events highlighted (adapted from Sepkoski, 1990).

End-Permian Mass Extinction (EPME) and post-extinction ooids

The End-Permian Mass Extinction (EPME) is considered the most severe mass extinction event since the beginning of the Phanerozoic eon (Benton, 1995; Erwin et al., 2002; Erwin, 2006; Payne et al., 2012; Burgess et al., 2014). According to previous estimates, 90% of marine species and 70% of terrestrial vertebrate species went extinct (Maxwell, 1992; Jin et al., 2000; Ward et al., 2005). Clapham et al. (2009) calculated a loss of marine invertebrate genera around 78%. The timing of the catastrophe is still debated, since it is unclear if it occurred as a unique cataclysmic event or as a gradual succession of minor events (Magaritz et al., 1988; Holser et al., 1989; Jin et al., 2000, Song et al 2013, Wang et al., 2014). New precise U-Pb dating on zircons allowed to determine that the extinction event lasted between 251.941 ± 0.037 and 251.880 ± 0.031 Mya (Burgess et al., 2014). Several studies point to extreme conditions in the oceans during this time period. Geological and geochemical data suggest high temperatures in the shallow tropical ocean (Joachimski et al., 2012; Sun et al., 2012), expansion of anoxic waters (Wignall & Twitchett, 1996; Isozaki, 1997; Brennecka et al., 2011; Lau et al., 2016), low sulfate concentrations (Kaiho et al., 2006; Luo et al., 2010), oceanic acidification (Knoll et al, 2007; Payne et al., 2007; Payne et al., 2010; Clarkson et al., 2015), metal or mercury poisoning (Kump et al., 2005; Grasby et al., 2020). These factors led to important changes in primary productivity (Rampino et al., 2005; Grasby et al., 2016). Bolide impacts, volcanism, ocean anoxia, seafloor and thermogenic methane emissions were proposed as causes of this event (Erwin, 1994; Racki & Wignall, 2005; Retallack & Jahre, 2008). Among these, the massive emplacement of flood basalt from the Siberian Traps Large Igneous Province (e.g., Dal Corso et al., 2022) is considered the most likely trigger of the extinction. This type of volcanism led to the rapid emission of large volumes of sulfate aerosols, CO_2 (Burgess et al., 2017) and further greenhouse gases generated by the thermal metamorphism between sedimentary host rocks and volcanic sills (Retallack & Jahren, 2008; Svensen et al., 2018; Callegaro et al., 2021; Sibik et al., 2021). According to Svensen et al. (2009) the consequent heating of evaporites and organic sediments in Tunguska Basin released enormous quantities of halocarbons and greenhouse gases in the atmosphere, such as CH_4 and CO_2 (>100,000 Gt of CO_2). This was clearly registered in the Tethys by $\delta 13C$ and $\delta 18O$ trends (Payne et al., 2004; Richoz 2006; Richoz et al., 2010; Korte & Kozur, 2010; Brand et al., 2012). For the Late Permian, further analyses on Ce anomaly and authigenic U redox indices highlighted oxic to dysoxic conditions in the seawater, at least in the western Tethys (Brennecka et al., 2011; Brand et al., 2012; Zhang et al., 2018). The consequences of the Siberian Traps emplacement lasted for all the Early Triassic (Payne et al. 2004; Horacek et al., 2007; Posenato, 2008; Stanley, 2009; Brayard et al., 2011; Chen & Benton, 2012). The biotic recovery was slow (~ 5 Myr) and contrasted by recurrent environmental perturbations (Wei et al., 2015). These perturbations caused minor extinctions in the Griesbachian/Dienerian (Kozur, 1998; Mei et al., 1999) and Smithian/Spathian boundary (Hallam & Wignall, 1997). They occurred together with strong climatic warming (probably due to persisting massive volcanism of the Siberian Traps) and deep-water anoxia in oceans (Li et al., 2013 and references therein). This scenario did not prevent microbial communities to develop and several peculiar "anachronistic facies" formed in this time interval (Sepkoski et al., 1991, Baud et al., 1997; 2007). The latter are mainly flat pebble conglomerates, microbialites, wrinkle structures, seafloor carbonate cement fans and ooids (Baud et al., 2007; Li et al., 2013 and references therein). In this scenario, globally spread abundant ooidal sediments spanned from immediately after the EPME time interval until the late Induan (Li et al., 2013; Li et al., 2015). These deposits formed primarily in shallow water settings between 30° N and 30° S latitude on the paleo-continent Pangea, mainly along the costs of Neo-Tethys, western Paleothethys and Eastern Tethys and within Panthalassa (Fig. 7).

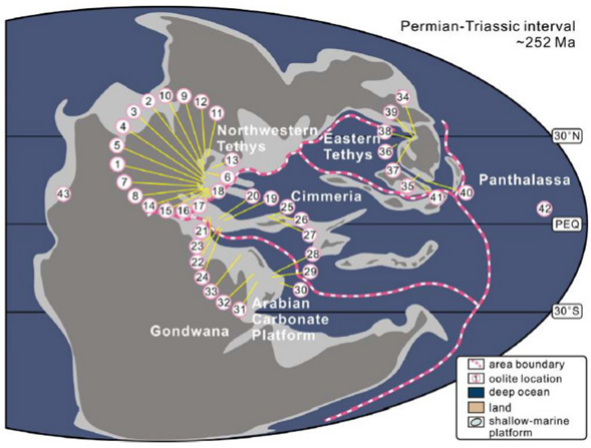

Fig. 7: Palaeogeographical distribution of oolites-bearing successions across the Permian-Triassic border. Numbers highlight each single locality (Retrieved from Li et al., 2015).

End-Triassic Mass Extinction (ETME) and post-extinction ooids

The Late Triassic (237-201 Ma) has been interpreted as an ice-free period, with high atmospheric pCO_2 levels (Price, 1999). Comparison between proxies (i.e., paleosols and stomatal index data) and modelling (i.e., Geoclim model) resulted in a pCO_2 estimate of >4000 ppm with a peak of 7000 ppm for Late Norian (Goddéris et al., 2008, 2014). These concentrations were tightly correlated with a 3–4 °C increase in Sea Surface Temperature (SST) associated with a global warming (McElwain et al., 1999; Knobbe & Schaller, 2018). At the same time, Earth experienced the end-Triassic Mass Extinction. It caused the disappearance of several invertebrate taxa, such as cnidarian and other reef builders (Stanley & Beauvais, 1994; Stanley, 1988, 2003), and molluscs (ammonoids, gastropods and bivalves) (Kiessling et al., 2007). It also prompted significant changes in plankton communities (Richoz et al., 2012). Unbuffered or acid-sensitive organisms were the most affected by the event (Hautmann 2004; Knoll et al., 2007; Clapham & Payne, 2011). Ecosystems were altered, as well as sedimentation patterns in basins (Hallam, 1996; van de Schootbrugge et al., 2013). In particular, a certain number of T-J marine sections registered a decrease or a lack of carbonate deposition (Greene et al., 2012b and references therein). The perturbation of the carbon cycle in the latest Rhaetian is also marked by three negative Carbon Isotope Excursions (CIEs) in the $\delta 13C$ record, due to an input of isotopically light carbon (e.g., Lindström et al., 2012, 2017, 2021; Dal Corso et al., 2014; Marzoli et al., 2018). The idea of a unique global extinction event is still debated and some authors consider it as product of more gradual and localized change, with no collapse of the terrestrial or marine food chain (Lucas & Tanner, 2018). Despite different interpretations of the event, the emplacement of the Central Atlantic Magmatic Province, CAMP, Marzoli et al., 1999), a basaltic Large Igneous Province (LIP) looks the most likely trigger for the extinction event (Marzoli et al., 2018). Its activity lasted between 600 ka and 1 Ma, peaking around 201 Ma (Schaltegger et al., 2008; Davies et al., 2017). A total estimated volume of 3 million km^3 of intruded and erupted magmas were released, together with a sudden input of volcanogenic gases such as water vapor, carbon, sulfur dioxide and halogens (Marzoli et al., 2018). A first peak in volcanic activity is correlated to the main extinction pulse and initial CIE and was characterized by relatively low temperature (350–500°C) heating of sedimentary rocks by intruding sills (Kaiho et al., 2022). A second extinction pulse, together with the main CIE, corresponds to higher temperatures and more effusive volcanism (Kaiho et al., 2022). The emplacement of the CAMP was large and rapid enough to cause an acidification event during the ETME time interval (Hautmann, 2004; Hautmann et al., 2008; Greene et al., 2012a; Kovács et al., 2022). This is revealed by the selective extinction of unbuffered or acid-sensitive taxa, the absence of reefal biota and changes in carbonate sedimentation in many marine boundary sections (Hautmann, 2004; Kiessling et al., 2007; Knoll et al., 2007; Hautmann et al., 2008; Kiessling, 2010; Clapham & Payne, 2011; Hillebrandt et al., 2013).

Even if anachronistic facies, such as abiotic seafloor precipitates, are not detected at the Triassic-Jurassic transition (Greene et al., 2012b), oolites occur in successions of the United Arab Emirates (Al-Suwaidi et al., 2016, Hönig et al., 2017; Ge et al. 2018, 2019), in the Northern Calcareous Alps (Austria, Felber et al., 2015) and in the Lombardy basin (Italy, Galli et al., 2007; Bachan et al., 2012) shortly after the extinction event. These oolites likely formed in a similar way than those at the Permian-Triassic boundary, as a consequence of the extinction of skeletal calcifiers (Al-Suwaidi et al., 2016).

Geological setting and study areas

Permian outcrops

Four different sections from the Italian Dolomites (south-eastern Alps) were selected along the Permian-Triassic boundary: Pufels/Bulla, Tesero, Seis/Siusi and Tramin/Termeno. The studied post-extinction oolites belong to a ca. 500 m thick mixed carbonate-siliciclastic ramp succession (Werfen Formation) that overlies the shallow-water/lagoonal environment of the upper Permian Bellerophon Formation. During the Permian-Triassic boundary interval, the Dolomites were part of the Pangea paleo-continent near the Equator, along the Paleo-Tethys Ocean. The Werfen Formation is Uppermost Permian-Lower Triassic in age (Changhsingian-Olenekian) and subdivided into nine members: Tesero Member, Mazzin Member, Andraz Member, Siusi Member, Gastropods Oolite Member, Campil Member, Val Badia Member, Cencenighe Member and San Lucano Member. The post-extinction ooid-bearing units belong to Tesero and Mazzin members.

Triassic outcrops

The three coeval sections that are the main object of study for the end-Triassic Mass Extinction are located in Wadi Milaha (Ras Al Khaimah Emirate, Musandam Peninsula, United Arab Emirates), on a mountain chain that exposes about a 3-km-thick succession of shallow water carbonates spanning from Permian to Cretaceous (Maurer et al., 2009). During the Late Triassic and the Early Jurassic, the area was an equatorial shallow-water carbonate platform (Ziegler, 2001) belonging to the Arabian shelf (Glennie et al, 1974), with more open-marine conditions to the north and terrigenous inputs coming from land areas in the south or south-west (Ziegler, 2001). The Arabian shelf was bordered by the Arabian shield in the southwest and the Tethys Ocean in the northeast (Maurer et al., 2008, Richoz et al., 2014). The studied Milaha and Ghalilah formations represent the Late Norian, Rhaetian and Early Jurassic time interval. The Milaha Formation is a 250 m thick succession of peritidal carbonates (limestone and dolostone). The Ghalilah Formation, which includes the Triassic-Jurassic Boundary is a mixed carbonate-siliciclastic unit subdivided into four members: the Asfal, Sumra, Sakhra and Shuba members.

Materials (and preparation of samples)

Sample collection

The material to be analysed in this project was collected in three field campaigns: two in the Ras Al Khaimah Emirate (2018 and 2020) and one in the Dolomites (2018). In the following table, collected samples and related localities are listed.

SECTION AND LOCALITY	EXTINCTION EVENT	NUMBER OF ROCK SAMPLES
PUFELS /BULLA (ITALY)	EPME	17
TESERO (ITALY)	EPME	14
SEIS/SIUSI (ITALY)	EPME	18
TRAMIN/TERMENO (ITALY)	EPME	13
WADI MILAHA (UAE)	ETME	317
WADI MILAHA 2 (UAE)	ETME	22
WADI MILAHA 3 (UAE)	ETME	18

Samples were prepared in different ways depending on type of analysis

Thin sections for optical microscope, elemental mapping and LA-ICP-MS analyses

Samples were cut in two halves with a Struers Discoplan-TS saw and the fresh surface was polished with a 600-grit diamond plate, mounted on a Struers Discoplan-25. From one of the halves a slice 5 mm thick was cut, with the dimension of a glass slide (about 28x48 mm). Each slab was glued on a pre-grinded and signed glass slide with a bicomponent epoxy resin, in a proportion 5:1 between Araldit DBF by ABIC Kemi and REN HY 956 by Huntsman. After drying the slabs one night

in an air oven at 50 °C, they were cut to 1 mm thick with a higher-precision Struers Discoplan-TS cutting and grinding machine. They were reduced to 40-35 µm thick using the same machine and then polished with a 1200 or 2000 grit diamond plate. To be analysed at LA-ICP-MS, thin sections were quickly pre-ablated to be perfectly clean.

Samples for SEM imaging

Small chips of rock were cut from each hand sample (5x5x8 mm). They were dried for one night in an air oven at 50 °C, then broken in two halves to obtain small cubes with a fresh surface (5x5x4 mm). Each small cube was mounted on a SEM stub with carbon tape. To avoid charging effects, the lateral sides of the sample were stained with silver paint. Samples were sputter coated with Pt/Pd (Cressington sputter coater 108 auto, 20 mA, 10 or 20 seconds).

Samples for stable isotopes ($\delta^{13}C_{carb}$ and $\delta^{18}O_{carb}$) analyses

Hand samples were polished with a 600-grit diamond plate and then micro-drilled to select specific rock components, avoiding visible fossils, veins or fractures. The powder material was then reacted with phosphoric acid to extract CO_2.

Methods

The analytical approach includes petrographic and geochemical methods.

Optical petrographic microscope

Thin sections were carefully described at the Department of Geology, Lund University, using an Olympus BX50 petrographic optical microscope, equipped with a digital camera (Olympus SC50). Samples lithology was classified according to the Dunham classification (Dunham, 1962) as revised by Embry & Klovan (1971) and Wright (1992). A description of Standard microfacies (SMF) was provided, following Wilson (1975) and Flügel (2010) and introducing new SMFs for specific rock assemblages. Moreover, we focused on the identification of several kinds of ooids and other coated grains, marking their size and stratigraphic distribution.

Point counting (modal analysis)

Thin sections were scanned with a Canon slide scanner at 4000 dpi and then point-counted with JMicroVision® software (Roduit, 2022). A random grid was used with spots having a default size of ten pixels (cf. Roduit, 2007). The number of points counted per section was 300 (cf. Galehouse, 1971).

SEM imaging (Scanning Electron Microscopy)

End-Triassic samples were imaged at the Department of Geology, Lund University, with a variable pressure Tescan Mira3 High Resolution Schottky FE-SEM equipped with an Oxford EDS detector, at 5 kV. End-Permian samples were instead imaged at the Department of Biology (Lund University) with a variable pressure Hitachi SU 3500 FE-SEM at 5 kV.

SEM elemental mapping (EDS and EBSD)

Elemental mapping of end-Triassic samples was done at the Department of Geology at Lund University with a variable pressure Tescan Mira3 High Resolution Schottky FE-SEM equipped with EDS (at 15 kV) and EBSD (at 20 kV) detectors. 30 μm thick thin sections were sputter coated with Pt/Pd (approximately 7 nm thickness) for EDS and treated in low-vacuum regime for EBSD, without any coating. Elemental and crystallographic mapping was realized with AZTEC® software. For EDS analyses, we consider a wide list of elements, which includes first Al, Ti, O, Ca, Si, Sr, Fe and Mg and additionally Ba, Mo, S, C, Br, Mn, Cd, V, Zn, U, Cl, N, Na, P, S, K, Pt, Pd as test-elements for some sample sites only.

LA-ICP-MS (Laser Ablation-Inductively Coupled Plasma-Mass Spectrometry)

The end-Permian and end-Triassic samples were processed at the Geology Department of Lund University using a Bruker Aurora-Elite Quadrupole ICP-MS. Analyses were performed on single spots that varied between 45x95 μm and 37x116 μm (constant area was kept). For each analysis, background collection took 30 s, while ablation was set to 30 s. Calibration was done with an internal standard where 43Ca was used, with the following concentrations: for the primary standard NIST SRM 610 (8.15 wt.%) and for three secondary standards: NIST SRM 612 (8.51 wt.%), NIST SRM 614 (8.50 wt. %), MACS-3 (37.7 wt. %). For primary and secondary standards, we calculated RSD% for each analysed element to evaluate analytical precision and accuracy of the measurements. Data reduction was done with Iolite software (Paton et al., 2011). The content of Ca in samples was set to 40 wt% by default and then corrected for Mg, Mn and Sr as carbonates and Al as oxide. We used the following formula for the correction: Wt% Ca*100/40+(Mg_ppm*$MgCO_3$_u/Mg_u+Mn_ppm*$MnCO_3$_u)/Mn_u+Al_ppm*Al_2O_3_u/ Al_2+ Sr_ppm*$SrCO_3$_u/ Sr_u)/10000, where u is referred to the atomic weight of the element. REE + Y concentrations were normalized against the PAAS (Post-Archean Australian Shale) standard (Taylor and McLennan, 1985).
Specific elements were selected for the analyses, with the purpose of investigating several paleoenvironmental variables. For instance, we monitor the bulk composition of ooids and other rock components at time of deposition ($MgCO_3$, Sr), the occurrence of detrital input (Al, Ti, V, P), the interaction of organic matter and/or bacteria within ooids (V, Ba, U, Zn, REE+Y), the incorporation of nutrients within ooids laminae (P), seawater oxygenation (Mn, V, U), the occurrence of redox conditions (REE+Y), early diagenetic processes (REE+Y, Mn).
Selected references: Brand and Veizer (1980); Sandberg (1983); German & Elderfield (1990); Smith et al. (1999); Algeo and Maynard (2004); Haley et al. (2004); Riding (2006); Tribovillard et al. (2006); Takahashi et al. (2005; 2007); Kamber & Webb (2007); Sánchez-Beristain & López-Esquivel Kranksith (2011); Li et al. (2013); Newsome et al. (2014); Li et al. (2017); Smrzka et al. (2019).

Stable isotopes ratio measurements

Stable isotopes analyses on end-Triassic samples were done partly at the Institute for Earth Sciences, University of Graz (Austria) with a ThermoFinnigan Kiel II autosampler connected online to a Thermo-Finnigan Delta V Plus mass spectrometer and partly at GeoZentrum, University of Erlangen-Nuremberg (Germany) with a Gasbench II autosampler connected online a Thermo-Finnigan Delta V Plus mass spectrometer. All values were then reported as per mil relative to V-PDB (Vienna- Pee Dee Belemnite) international standard. Standard deviations (1 σ) from NBS19, IAEA-CO9, NBS18 and an in-house standard were less than ± 0,15 ‰ and ± 0,25 ‰ for $\delta^{13}C$ and $\delta^{18}O$, respectively.

Discussion of results

Paper I

Analysis of the Wadi Milaha sections provided new insights into the geochemistry and sedimentology of the Late Triassic-Early Jurassic. The $\delta^{13}C_{carb}$ record presented in this paper shows a negative excursion for the mid-Norian, which however could reflect a local signal due to water restriction in this shallow setting. Across the Norian-Rhaetian Boundary (NRB), the $\delta^{13}C_{org}$ record is very stable and in agreement with the data of Kovács (2021). The NRB itself was well constrained due to findings of the conodonts *Epigondolella bidentata* and *Misikella posthernsteini* and the ammonoid *Neotibetites* sp. The C and O isotope data retrieved from post-ETME beds constitute a robust, non-diagenetically overprinted record, although the late Triassic *marshi* CIE is lacking. We demonstrated the presence of a stratigraphic hiatus of unknown extent at the extinction level, supported by a clear erosional surface. This level displays a substantial change in facies from pre-extinction coral-rich rudstones/floatstones to post-extinction less fossiliferous packstone/grainstones with high abundance of ooids. The TJB interval in Wadi Milaha section preserves the same transgressive trend as other Hettangian sections around the world. The features of this transgression can be linked to an abrupt demise of the carbonate factory at the ETME and motivate an extension of the "unreefing" model by Pálfy et al. (2021) into southern latitude platforms like the Arabic platform. Our focus on the coated grains deposited after the ETME resulted in a new morphological classification. The coarsening-upward trend of oolitic cycles C1, C2 and C3 traced by Ge et al. (2018, 2019) is confirmed only for cycle C1, while we addressed the poor preservation and deformation of ooids in cycle C2 as strictly local, as well as the micritic appearance of ooids and the siliciclastic input in cycle C3. We consider the extreme variability of post-extinction ooids a product of both water chemistry (redox conditions, nutrients supply, rate of dissolved carbon in marine water) and local sedimentological (wave energy) factors. In the light of these final considerations, we discussed the role of the two variables (chemistry vs. sedimentological) in paper II, providing geochemical investigations at the ooids laminae scale.

Paper II

Detailed petrographical and geochemical investigation of ooids and coated grains deposited in the early aftermath of the end-Triassic mass-extinction (ETME) at Wadi Milaha support an original precipitation of low-Mg calcite during a time interval corresponding to the Aragonite Sea II. Our data, which implement the already existing datasets on the "Aragonite Sea-Calcite Sea" problem, suggest that the shift from Aragonite Sea II to Calcite Sea II occurred earlier than previously believed. Alternatively, our results point toward a strong depletion in sulfate, which could have as well favoured calcite over aragonite deposition. The postulated increase in anoxic area in the direct aftermath of the mass-extinction, with an increase in sulfide burial could have led to such a dramatic decrease in seawater sulfate. Further study of Rhaetian ooids will be needed to define the exact duration (limited to the ETME aftermath or already starting in the Rhaetian?) and location (regional or global scale phenomenon?) of this brief interval of calcitic precipitation. An increase in detrital elements (Al, Ti, V, Cr, Ni, Ba) is observed in superficially coated grains belonging to the earliest aftermath of the ETME, reflecting a sudden pulse of detrital material shortly after the extinction. The best developed, least micritized and morphologically highly diverse ooids correspond to a stratigraphic interval with unusually high P and associated ΣREE+Y. We propose that the acidification event linked to the ETME transformed the carbonate platform into a ramp geometry (the "unreefing" model of Pálfy et al., 2021), allowing deep water, charged in P to more easily reach the shallow-water platform. These nutrient-rich and slightly oxygen depleted waters may have favoured ooids accretion and may as well explain the Mn and Ce anomaly signal of the radial ooids, which indicate local dysoxia in the quieter environment of the shoals. These final considerations show how this study can be a new step towards the understanding of the oscillations of the "Aragonite Sea-Calcite Sea" trend, both on a regional and global scale, and also highlight the crucial role of ooids and coated grains in tracking post-extinction extreme environmental conditions in the oceans.

Paper III

This paper provided a detailed petrographical and geochemical investigation of ooids and coated grains de-

posited in the early aftermath of the end-Permian Mass Extinction (EPME) in four sections of the Dolomites (Southern Alps, Italy). These sections were affected by early diagenetic recrystallization or early dolomitization. The recrystallization kept the elements linked to Al, increased Mn and decreased all other elements. This trend is stronger in coarser recrystallization patterns. Early dolomitization retains as well the Al group and Mn, and decrease the ratio of all other elements. Recrystallization and early dolomitization prevent thus any solid conclusion on the mineralogy of precipitation of the ooids studied. Fewer environmental factors during the time of deposition can be retrieved from this dataset in comparison to the well-preserved Emirati ooids. However, we could demonstrate an enrichment in detrital element rapidly after the extinction event. This could be the results of a rapid transgression and/or of catastrophic soil erosion in the extinction aftermath. This interval with increased elements derived from chemical weathering is shorter than the interval showing increased terrestrial biomarkers and pollen. It could thus not sustain a long-lasting anoxia through eutrophication as cause of the second extinction level as sometime hypothesized.

Conclusions and future perspectives

This dissertation shed new light on how multi-technique petrographical and geochemical investigation can be applied to characterize post-extinction coated grains. However, the results presented in the papers leave some open questions for future research.

Paper I and II

The implementation of the existing global inventory of post-ETME ooids contributes to the on-going debate on the exact temporal location of the calcite interval in Aragonite Sea II-Calcite Sea II transition. The high-resolution scale at which geochemical analyses were performed on ooids and other rock components was new for the Triassic-Jurassic sections of the Arabian Peninsula. It could be applied in the future to the characterization of other coeval/comparable sections in the same time interval. However, few relevant elements were excluded from the analyses with LA-ICP-MS, due to limitations of the instrumentation: Fe, Si and some REE (Pm, Tb, Ho and Tm). Si was excluded because it has a high baseline due to the presence of glass in the instrumentation, that results in higher detection limit; it is the same for Ni, where the presence of nickel cones in the ICP-MS rises its baseline and low concentrations of Ni are more difficult to detect. Fe was not included because its isotopes ^{57}Fe, ^{56}Fe and ^{54}Fe show interferences with those of Ca, O, H, Ar and Cr, limiting a correct acquisition of the chemical signal. Some of the REE were not included to shorten the list of analyzed elements, as the higher the number the lower the accuracy of the measurements. This prevented ΣREE+Y to be compared as absolute value with previous publications, but we used them in correlation with other elements only. Alternative methods can be used to acquire these "problematic" elements. As Fe is a quencher in carbonate rocks for luminescence, it could be useful to acquire some cathodoluminescence data, for a first qualitative evaluation. Then, limiting the number of analyzed elements, SIMS could be used to quantify the concentration of Si, Fe and Ni. This instrument does not imply the use of plasma, as cause of the interference process in LA-ICP-MS. A complete retrieval of REE at LA-ICP-MS could be easier with a second dedicated run of analyses and a diversification of the acquisition mode of other elements. Another aspect that could be worth deepening is the gain of higher resolution images and chemical maps to acquire through synchrotron facilities. This will be a pioneering approach in ooids studies. This kind of data could potentially help the reconstruction of post-depositional features such as microborings, to correlate their distribution with that of micronutrients in the ooids laminae.

On another side, the dataset of oolites presented in both papers would need to be widened, including Rhaetian ooids to determine the exact duration and location of the calcite interval. The analyses of several major and trace elements in the ooids revealed how phenomena at the local scale (e.g., major detrital input in the immediate aftermath of the extinction event) can have an important role in testing and updating formational models at the global scale, such as the one of Pálfy et al. (2021). The detailed logging and sampling of the Wadi Milaha section provided the longest continuous $\delta^{13}C_{carb}$ record in one single section with biostratigraphic control until now, and therefore it could be a good reference for future publications; moreover, our focus on mapping lateral stratigraphical and sedimentological variability of the Wadi Milaha succession improved our understanding of the depositional processes and helped discriminating between primary features of the ooids and post-deposition imprint.

Paper III

The study of post-EPME ooids in the Italian Dolomites tooks a further step in the application of the multi-technique approach we had already discussed in papers I and II. The recrystallization and dolomitization processes that affected the documented sections prevented the possibility to retrieve the original geochemical signature of the depositional environment (i.e., post-extinction seawater). However, it was still possible to carefully describe the morphology of different recrystallization patterns in ooids cortices and nuclei, providing a detailed mapping of the distribution of major and trace elements according to the kind of pattern and process (recrystallization in calcite vs. dolomitization) occurring during the diagenesis. We showed it is still meaningful to acquire geochemical data on diagenetically altered samples and coated grains, as it can be used as a protocol to treat samples from other localities, stressing the role of more conservative elements to trace back the original signature of seawater. The provided geochemical analyses have some limitations that could be solved as illustrated above for paper II. In the light of these considerations, a natural implementation of the present paper would be to collect and characterize same age oolites with a comparable recrystallization pattern. This is the case of, for instance, Cimmerian sections from Turkey, also characterized by recrystallized post-EPME ooids (Li et al., 2015).

In conclusion, we think that future studies on ooids formed during time periods of extreme environmental conditions will benefit from the wide-perspective analytical protocol defined by this dissertation work. The issue of diagenetic alteration is still currently seen as a big obstacle to reliable geochemical analyses, but hopefully we here show how this kind of samples are worth to investigate.

Authors Contribution

	Paper I	Paper II	Paper III
Study design	S. Richoz and I. Urban	S. Richoz and I. Urban	S. Richoz and I. Urban
Data collection			
Fieldwork	I. Urban, S. Richoz, I. Demangel, Z. Kovács, L. Krystyn, S. Lernpeiss, G. Gradwohl and F. Maurer	I. Urban and S. Richoz	I. Urban
Sampling	I. Urban, S. Richoz, Demangel, Z. Kovács, L. Krystyn, S. Lernpeiss, G. Gradwohl and F. Maurer	I. Urban and S. Richoz	I. Urban
Section description	I. Urban, S. Richoz, Demangel, Z. Kovács, L. Krystyn, S. Lernpeiss, G. Gradwohl and F. Maurer	I. Urban and S. Richoz	I. Urban
Data analyses			
Petrographic analysis of thin sections	I. Urban (including oolitic interval), L. Krystyn, S. Lernpeiss, G. Gradwohl and F. Maurer	I. Urban	I. Urban
Modal analysis	I. Urban		
Fossil determination	L. Krystyn and F. Maurer		
Calcareous nannofossils content	I. Demangel		
SEM imaging	I. Urban	I. Urban	I. Urban
SEM elemental mapping (EDS and EBSD)		I. Urban	I. Urban
LA-ICP-MS (including data reduction and error analyses)		I. Urban and T. Naeraa	I. Urban and T. Naeraa
Stable isotopes ratio measurements	I. Urban (Wadi Milaha) and S. Lernpeiss, G. Gradwohl (Wadi Bih)		
Writing: original draft	I. Urban	I. Urban	I. Urban
Writing: review and editing	All authors	All authors	All authors
Design and preparation of figures	I. Urban, I. Demangel, G. Gradwohl, S. Lernpeiss, S. Richoz	I. Urban and S. Richoz	I. Urban and I. Demangel

Populärvetenskaplig sammanfattning

Om du tar en handfull sand från en av Bahamas tropiska stränder, kommer du att se hur varje korn är vitaktigt och runt eller ovalt till formen, som ett litet ägg. Dessa korn kallas "ooider" och är mycket små (mindre än 2 mm) och består av kalciumkarbonat (kalk). De består av exceptionellt tunna, koncentriska lager på lager runt en kärna. Ooider är en del av jordens historia sedan den sen-arkeiska tidsperioden för ungefär 2800-2500 miljoner år sedan. När de genom geologiska processer kittas ihop till en bergart bildar de en kalksten som kallas "oolit". Ooliter är potentiellt utmärkta arkiv för att studera jordens tidigare miljöer. Den forskning som presenteras här baseras på marina ooider, alltså de ooider som bildats i grunda havsområden i Jordens urtid. Det har visat sig att ooider tenderar att bildas i onormalt omfattande utsträckning och bilda tjocka sedimentavlagringar direkt efter omfattande kriser i biologisk mångfald, så kallade "massutdöenden". Sådana katastrofala händelser är ofta följden av extrema klimatförhållanden, som ledde till att en betydande del av Jordens arter försvann, både i haven och på kontinenterna. Det mest omfattande massutdöendet i Jordens historia ägde rum vid slutet av den permiska tidsperioden för omkring 251 miljoner år sedan. Syftet med denna avhandling är att förstå och dokumentera de specifika kemiska och fysikaliska förhållanden som rådde i havsvattnet efter utdöendena och förstå dess påverkan för miljön och djurlivet. Vi fokuserade på två massutdöenden, det vis slutet av perm och det som avslutar tidsperioden trias för cirka 201 miljoner år sedan. För det förstnämnda utdöendet beskrev vi ooider från Dolomiterna i Italien och för det senare från Förenade Arabemiraten, med hjälp av flera avancerade analytiska tekniker. Genom att använda optisk mikroskopi och svepelektronmikroskopi beskrev vi noggrant ooidernas interna struktur och dokumenterade hur olika typer och storlekar av ooider samvarierade i tid omedelbart efter utdöendena. Vi analyserade även kemisk information från ooiderna, såväl som från andra komponenter i bergartsproverna, genom att använda elementanalys i svepelektronmikroskop och laserablation kopplad till masspektrometri. För att vidga vårt perspektiv med avseende på miljökonsekvenserna av utdöenden beskriver vi mer omfattande de sedimentära bergartslager som avsattes direkt efter utdöendet i slutet av trias i Wadi Milaha i Förenade Arabemiraten. Där analyserar vi även kolets och syrets stabila isotoper ($\delta^{13}C_{carb}$ och $\delta^{18}O_{carb}$). De paleomiljödata vi samlat in lägger till ny information om hur haven reagerade på extrema händelser i Jordens urtida atmosfär och biosfär. Idag står mänskligheten inför nya utmaningar i det globala klimatet, vilket senast konstaterades under 2023 av IPCC (Intergovernmental Panel on Climate Change): "Human activities, principally through emissions of greenhouse gases, have unequivocally caused global warming, with global surface temperature reaching 1.1°C above 1850–1900 in 2011–2020". Att jämföra konsekvenserna av mänsklig påverkan på nuvarande och framtida klimat med tidigare naturliga händelser, som orsakade omfattande kriser för den biologiska mångfalden, kan bidra till att fördjupa vår kunskap och för att vidta begränsningsåtgärder i en av de viktigaste frågorna under detta århundrade.

References

Algeo, T. J., & Maynard, J. B., 2004. Trace-element behavior and redox facies in core shales of Upper Pennsylvanian Kansas-type cyclothems. Chemical geology, 206(3-4), 289-318. https://doi.org/10.1016/j.chemgeo.2003.12.009

Alroy, J., Aberhan, M., Bottjer, D. J., Foote, M., Fürsich, F. T., Harries, P. J., Hendy, A. J. W., Holland, S. M., Ivany, L. C., Kiessling, W., Kosnik, M. A., Marshall, C. R., McGowan, A. J., Miller, A. I., Olszewski, T. D., Patzkowsky, M. E., Peters, S. E., Villier, L., Wagner, P. J., Bonuso, N., Borkow, P. S., Brenneis, B., Clapham, M. E., Fall., L. M., Ferguson, C. A., Hanson, V. L., Krug, A. Z., Layou, K. M., Leckey, E. H., Nürnberg, S., Powers, C. M., Sessa, J. A., Simpson, C., Tomašových, A., & Visaggi, C. C., 2008. Phanerozoic trends in the global diversity of marine invertebrates. Science, 321(5885), 97-100. doi:10.1126/science.1156963

Al-Suwaidi, A. H., Steuber, T., & Suarez, M. B., 2016. The Triassic-Jurassic boundary event from an equatorial carbonate platform (Ghalilah Formation, United Arab Emirates). Journal of the Geological Society, 173(6), 949-953. doi:10.1144/jgs2015-102

Anderson, N.T., Cowan, C.A., & Bergmann, K.D., 2020. A case for the growth of ancient ooids within the sediment pile. J. Sediment. Res. 90 (8), 843–854.

Ariztegui, D., Plee, K., Farah, R., Menzinger, N., & Pacton, M., 2012. Bridging the gap between biological and sedimentological processes in ooid formation: Crystalizing FA FOREL's vision. Archives des Sciences, 65, 93-102.

Bachan, A., van de Schootbrugge, B., Fiebig, J., McRoberts, C.A., Ciarapica, G., Payne, J. L., 2012. Carbon cycle dynamics following the end-Triassic mass extinction: constraints from paired $\delta^{13}C_{carb}$ and $\delta^{13}C_{org}$ records. Geochem. Geophys. Geosyst. 13 (9).

Batchelor, M. T., Burne, R. V., Henry, B. I., Li, F., & Paul, J., 2018. A biofilm and organomineralisation model for the growth and limiting size of ooids. Scientific reports, 8(1), 559.

Bathurst, R. G., 1972. Carbonate sediments and their diagenesis (Vol. 12): Elsevier.

Baud, A., Cirilli, S., & Marcoux, J., 1997. Biotic response to mass extinction: The lowermost Triassic microbialites. Facies, 36, 238-242.

Baud, A., Richoz, S., & Pruss, S., 2007. The lower Triassic anachronistic carbonate facies in space and time. Global and Planetary Change, 55(1-3), 81-89. doi:10.1016/j.gloplacha.2006.06.008

Baumgartner, L. K., Reid, R. P., Dupraz, C., Decho, A. W., Buckley, D. H., Spear, J. R., Przekop, K. M., & Visscher, P. T., 2006. Sulfate reducing bacteria in microbial mats: changing paradigms, new discoveries. Sedimentary Geology, 185(3-4), 131-145.

Beaupré, S. R., Roberts, M. L., Burton, J. R., & Summons, R. E., 2015. Rapid, high-resolution ^{14}C chronology of ooids. Geochimica et Cosmochimica Acta, 159, 126-138.

Benton, M. J., 1995. Diversification and extinction in the history of life. Science, 268(5207), 52-58. doi:10.1126/science.7701342

Brand, U., & Veizer, J., 1980. Chemical diagenesis of a multicomponent carbonate system; 1, Trace elements. Journal of Sedimentary Research, 50(4), 1219-1236.

Brand, U., Posenato, R., Came, R., Affek, H., Angiolini, L., Azmy, K., & Farabegoli, E., 2012. The end-Permian mass extinction: A rapid volcanic CO_2 and CH_4-climatic catastrophe. Chemical Geology, 322, 121-144. doi:10.1016/j.chemgeo.2012.06.015

Brayard, A., Vennin, E., Olivier, N., Bylund, K. G., Jenks, J., Stephen, D. A., Bucher, H., Hofmann, R., Goudemand, N., & Escarguel, G., 2011. Transient metazoan reefs in the aftermath of the end-Permian mass extinction. Nature Geoscience, 4(10), 693-697. doi:10.1038/ngeo1264

Brennecka, G. A., Herrmann, A. D., Algeo, T. J., & Anbar, A. D., 2011. Rapid expansion of oceanic anoxia immediately before the end-Permian mass extinction. Proceedings of the National Academy of Sciences of the United States of America, 108(43), 17631-17634. doi:10.1073/pnas.1106039108

Burgess, S. D., Bowring, S., & Shen, S. Z., 2014. High-precision timeline for Earth's most severe extinction (vol 111, pg 3316, 2014). Proceedings of the National Academy of Sciences of the United States of America, 111(13), 5060-5060. doi:10.1073/pnas.1403228111

Burgess, S.D., Muirhead, J.D., & Bowring, S.A., 2017. Initial pulse of Siberian Traps sills as the trigger of the end-Permian mass extinction: Nature Communications, v. 8, 164, https://doi .org/10.1038/s41467-017-00083-9.

Callegaro, S., Svensen, H. H., Neumann, E. R., Polozov, A. G., Jerram, D. A.,

Deegan, F. M., Planke, S., Shiganova, O. V., Ivanova, N.A., & Melnikov, N.V., 2021. Geochemistry of deep Tunguska basin sills, Siberian Traps: correlations and potential implications for the end- Permian environmental crisis. Contribut. Mineral. Petrol. 176, 49 (2021). https://doi .org/10.1007/s00410-021-01807-3

Carozzi, A. V., 1960. Microscopic sedimentary petrography.

Chen, Z.-Q., & Benton, M. J., 2012. The timing and pattern of biotic recovery following the end-Permian mass extinction. Nature Geoscience, 5(6), 375.

Clapham, M. E., & Payne, J. L., 2011. Acidification, anoxia, and extinction: A multiple logistic regression analysis of extinction selectivity during the Middle and Late Permian. Geology, 39(11), 1059-1062. doi:10.1130/g32230.1

Clapham, M. E., Shen, S. Z., & Bottjer, D. J., 2009. The double mass extinction revisited: reassessing the severity, selectivity, and causes of the end-Guadalupian biotic crisis (Late Permian). Paleobiology, 35(1), 32-50. doi:10.1666/08033.1

Clarkson, M., Kasemann, S., Wood, R., Lenton, T., Daines, S., Richoz, S., Ohnemueller, F., Meixner, A., Poulton, S. W., & Tipper, E., 2015. Ocean acidification and the Permo-Triassic mass extinction. Science, 348(6231), 229-232.

Dal Corso, J., Marzoli, A., Tateo, F., Jenkyns, H.C., Bertrand, H., Youbi, N., Mahmoudi, A., Font, E., Buratti, N., Cirilli, S., 2014. The dawn of CAMP volcanism and its bearing on the end-Triassic carbon cycle disruption. J. Geol. Soc. Lond. 171, 153–164.

Dal Corso, J., Song, H., Callegaro, S., Chu, D., Sun., Y., Hilton, J., Grasby, S.E., Joachimiski, M.M., & Wignall, P. B., 2022. Environmental crises at the Permian–Triassic mass extinction. Nature Reviews Earth and Environment 3, 197-214. https://doi.org/10.1038/ s43017-021-00259-4.

Davies, J. H. F. L., Marzoli, A., Bertrand, H., Youbi, N., Ernesto, M., & Schaltegger, U., 2017. End-Triassic mass extinction started by intrusive CAMP activity. Nature communications, 8, 15596. doi:10.1038/ncomms15596

Davies, P. J., Bubela, B., & Ferguson, J., 1978. The formation of ooids. Sedimentology, 25(5), 703-730.

Diaz, M. R., Van Norstrand, J. D., Eberli, G. P., Piggot, A. M., Zhou, J., & Klaus, J. S., 2014. Functional gene diversity of oolitic sands from Great Bahama Bank. Geobiology, 12(3), 231-249.

Diaz, M. R., Eberli, G. P., Blackwelder, P., Phillips, B., & Swart, P. K., 2017. Microbially mediated organomineralization in the formation of ooids. Geology, 45(9), 771-774.

Duguid, S. M., Kyser, T. K., James, N. P., & Rankey, E. C., 2010. Microbes and ooids. Journal of Sedimentary Research, 80(3), 236-251.

Dunham, R. J., 1962. Classification of carbonate rocks according to depositional textures. in: Classification of Carbonate Rocks (W.E. Ham, Editor). Mem. Am. Assoc. Petrol. Geol. Pp. 183.

Dupraz, C., & Visscher, P. T., 2005. Microbial lithification in marine stromatolites and hypersaline mats. Trends in microbiology, 13(9), 429-438.

Dupraz, C., Reid, R. P., Braissant, O., Decho, A. W., Norman, R. S., & Visscher, P. T., 2009. Processes of carbonate precipitation in modern microbial mats. Earth-Science Reviews, 96(3), 141-162.

Embry, A.F., & Klovan, J.E., 1971. A late Devonian reef tract on northeastern Banks Island, NWT. Bull. Can. Petrol. Geol. 19 (4), 730–781.

Erwin, D. H., 1994. THE PERMO-TRIASSIC EXTINCTION. Nature, 367(6460), 231-236. doi:10.1038/367231a0

Erwin, D. H., Bowring, S. A., & Yugan, J., 2002. End-permian mass extinctions: A review. In C. Koeberl & K. G. MacLeod (Eds.), Catastrophic Events and Mass Extinctions: Impacts and Beyond (Vol. 356, pp. 363-383).

Erwin, D.H., 2006. Extinction: How Life on Earth Nearly Ended 250 Million Years Ago. Princeton, NJ: Princeton Univ. Press. 306 pp.

Felber, R., Weissert, H.J., Furrer, H., Bontognali, T.R., 2015. The Triassic-Jurassic boundary in the shallow-water marine carbonates from the western Northern Calcareous Alps (Austria). Swiss J. Geosci. 108 (2), 213–224.

Flügel, E., 2010. Microfacies of carbonate rocks: analysis, interpretation and application (Vol. 976, p. 2004). Berlin: springer.https://doi.org/10.1007/978-3-642-03796-2

Flügel, E., 2012. Microfacies analysis of limestones: Springer Science & Business Media.

Galehouse, J.S., 1971. Point counting. In: Carver, R.E. (Ed.), Procedures in Sedimentary Petrology: New York. John Wiley and Sons, pp. 385–407.

Galli, M.T., Jadoul, F., Bernasconi, S.M., Cirilli, S., Weissert, H., 2007. Stratigraphy and palaeoenvironmental analysis of the Triassic-Jurassic transition in the western Southern Alps (Northern Italy). Palaeogeogr. Palaeoclimatol. Palaeoecol. 244 (1–4), 52–70.

Ge, Y., Shi, M., Steuber, T., Al-Suwaidi, A.H., Suarez, M.B., 2018. Environmental change during the Triassic-Jurassic boundary interval of an equatorial carbonate platform: sedimentology and chemostratigraphy of the Ghalilah Formation, United Arab Emirates. Palaeogeogr. Palaeoclimatol. Palaeoecol. 502, 86–103.

Ge, Y., Al-Suwaidi, A.H., Shi, M., Li, Q., Morad, S., Steuber, T., 2019. Short-term variation of ooid mineralogy in the Triassic-Jurassic boundary interval and its environmental implications: Evidence from the equatorial Ghalilah Formation, United Arab Emirates. Global Planet. Change 182, 103006.

German, C. R., & Elderfield, H., 1990. Application of the Ce anomaly as a paleoredox indicator: the ground rules. Paleoceanography, 5(5), 823-833. doi:10.1029/PA005i005p00823

Glennie, K.W., Boeuf, M.G.A., Huges-Clarke, M.W., Moody-Stuart, M., Pilaar, W.F.H., Reinhardt, B.M., 1974. Geology of the Oman Mountains. The Hague, Martinus Nijhoff, Verhandelingen Koninklijk Nederlands Geologie en Mijnbouw Genootschap, 31:1–423.

Goddéris, Y., Donnadieu, Y., de Vargas, C., Pierrehumbert, R. T., Dromart, G., & van de Schootbrugge, B., 2008. Causal or casual link between the rise of nannoplankton calcification and a tectonically-driven massive decrease in Late Triassic atmospheric CO_2?. Earth and Planetary Science Letters, 267(1-2), 247-255.

Godderis, Y., Donnadieu, Y., Le Hir, G., Lefebvre, V., & Nardin, E., 2014. The role of palaeogeography in the Phanerozoic history of atmospheric CO_2 and climate. Earth-Science Reviews, 128, 122-138. doi:10.1016/j.earscirev.2013.11.004

Grasby, S. E., Beauchamp, B., & Knies, J., 2016. Early Triassic productivity crises delayed recovery from world's worst mass extinction. Geology, 44(9), 779-782. doi:10.1130/g38141.1

Grasby, S.E., Liu, X., Yin, R., Ernst, R.E., & Chen, Z., 2020. Toxic mercury pulses into late Permian terrestrial and marine environments: Geology, 48(8), p. 830-833, https://doi .org/10.1130/G47295.1

Greene, S.E., Bottjer, D.J., Corsetti, F.A., Berelson, W.M., Zonneveld, J.P., 2012a. A subseafloor carbonate factory across the Triassic-Jurassic transition. Geology 40 (11), 1043–1046.

Greene, S. E., Martindale, R. C., Ritterbush, K. A., Bottjer, D. J., Corsetti, F. A., & Berelson, W. M., 2012b. Recognising ocean acidification in deep time: An evaluation of the evidence for acidification across the Triassic-Jurassic boundary. Earth-Science Reviews, 113(1-2), 72-93.

Gygi, R., 1981. Oolitic iron formations: marine or not marine. Eclogae Geologicae Helvetiae, 74(1), 233-254.

Haley, B. A., Klinkhammer, G. P., & McManus, J., 2004. Rare earth elements in pore waters of marine sediments. Geochimica et Cosmochimica Acta, 68(6), 1265-1279. doi:10.1016/j.gca.2003.09.012

Hallam, A., 1996. Major bio-events in the Triassic and Jurassic (pp. 265-283). Springer Berlin Heidelberg.

Hallam, A., & Wignall, P. B., 1997. Mass extinctions and their aftermath. Oxford University Press, UK.

Hardie, L. A., 1996. Secular variation in seawater chemistry: An explanation for the coupled secular variation in the mineralogies of marine limestones and potash evaporites over the past 600 my. Geology, 24(3), 279-283. https://doi.org/10.1130/0091-7613(1996)024<0279:SVISCA>2.3.CO;2

Hardie, L. A., 2003. Secular variations in Precambrian seawater chemistry and the timing of Precambrian aragonite seas and calcite seas. Geology, 31(9), 785-788.

Hautmann, M., 2004. Effect of the end-Triassic CO2 maximum on carbonate sedimentation and marine mass extinction. Facies 50, 257–261. https://doi.org/10.1007/s10347-004-0020-y

Hautmann, M., Benton, M.J., Tomaˇsových, A., 2008. Catastrophic ocean acidification at the Triassic-Jurassic boundary. Neues Jahrb. Geol. Palaontol. Abh. 249, 119–127.

Hillebrandt, A.V., Krystyn, L., Kürschner, W.M., Bonis, N.R., Ruhl. M., Richoz, S., Urlichs, M., Bown, P.R., Kment, K., McRoberts, CH., Simms, M. & Tomasovych, A., 2013: The Global Stratotype Sections and Point (GSSP) for the base of the Jurassic Period at Kuhjoch (Karwendel Mountains, Northern Calcareous Alps, Tyrol, Austria). – Episodes, 36, 162–198, Ottawa.

Holser, W. T., Schönlaub, H. P., Attrep, M., Boeckelmann, K., Klein, P., Magaritz, M., Orth, C., J., Fenninger, A., Jenny, C., Kralik, M., Mauritsch, H., Pak, E., Schramm, J.-M., Stattegger, K., & Schmoller, R., 1989. A unique geochemical record at the Permian Triassic boundary. Nature, 337(6202), 39-44. doi:10.1038/337039a

Horacek, M., Brandner, R., & Abart, R., 2007. Carbon isotope record of the P/T boundary and the Lower Triassic in the Southern Alps: Evidence for rapid changes in storage of organic carbon. Palaeogeography Palaeoclimatology Palaeoecology, 252(1-2),

347-354. doi:10.1016/j.palaeo.2006.11.049

Hönig, M.R., John, C.M., Manning, C., 2017. Development of an equatorial carbonate platform across the Triassic-Jurassic boundary and links to global palaeoenvironmental changes (Musandam Peninsula, UAE/Oman). Gondw. Res. 45, 100–117.

IPCC (2023): Summary for Policymakers.https://www.ipcc.ch/sr15/ (accessed 26 March 2023)

Isozaki, Y., 1997. Permo-Triassic boundary superanoxia and stratified superocean: Records from lost deep sea. Science, 276(5310), 235-238. doi:10.1126/science.276.5310.235

Jin, Y. G., Wang, Y., Wang, W., Shang, Q. H., Cao, C. Q., & Erwin, D. H., 2000. Pattern of marine mass extinction near the Permian-Triassic boundary in South China. Science, 289(5478), 432-436. doi:10.1126/science.289.5478.432

Joachimski, M. M., Lai, X. L., Shen, S. Z., Jiang, H. S., Luo, G. M., Chen, B., Chen, J., & Sun, Y. D., 2012. Climate warming in the latest Permian and the Permian-Triassic mass extinction. Geology, 40(3), 195-198. doi:10.1130/g32707.1

Kaiho, K., Kajiwara, Y., Chen, Z. Q., & Goljan, P., 2006. A sulfur isotope event at the end of the Permian. Chemical Geology, 235(1-2), 33-47. doi:10.1016/j.chemgeo.2006.06.001

Kaiho, K., Tanaka, D., Richoz, S., Jones, D.S., Saito, R., Kameyama, D., Ikeds, M., Takahashi, S., Aftabuzzuman, M.d., & Fujibayashi, M., 2022. Volcanic temperature changes modulated volatile release and climate fluctuations at the end-Triassic mass extinction. Earth Planet. Sci. Lett. 579, 117364 https://doi.org/10.1016/j.epsl.2021.117364.

Kamber, B. S., & Webb, G. E., 2007. Transition metal abundances in microbial carbonate: a pilot study based on in situ LA-ICP-MS analysis. Geobiology, 5(4), 375-389. doi:10.1111/j.1472-4669.2007.00129.x

Kiessling, W., 2010. Reef expansion during the Triassic: Spread of photosymbiosis balancing climatic cooling. Palaeogeography, Palaeoclimatology, Palaeoecology, 290(1-4), 11-19. https://doi.org/10.1016/j.palaeo.2009.03.020

Kiessling, W., Aberhan, M., Brenneis, B., & Wagner, P. J., 2007. Extinction trajectories of benthic organisms across the Triassic–Jurassic boundary. Palaeogeography, Palaeoclimatology, Palaeoecology, 244(1-4), 201-222.

Knobbe, T.K., & Schaller, M.F., 2018. A tight coupling between atmospheric pCO2 and sea- surface temperature in the Late Triassic. Geology 46 (1), 43–46.

Knoll, A. H., Bambach, R. K., Payne, J. L., Pruss, S., & Fischer, W. W., 2007. Paleophysiology and end-Permian mass extinction. Earth and planetary science letters, 256(3-4), 295-313. doi:10.1016/j.epsl.2007.02.018

Korte, C., & Kozur, H. W., 2010. Carbon-isotope stratigraphy across the Permian-Triassic boundary: A review. Journal of Asian Earth Sciences, 39(4), 215-235. doi:10.1016/j.jseaes.2010.01.005

Kovács, Z., 2021. The origin of pelagic calcification and its influence on seawater chemistry. PhD Thesis, 294 p. Graz University.

Kovács, Z., Demangel, I., Schmitt, A.-D., Gangloff, S., Baldermann, A., Hippler, D., Krystyn, L. & Richoz, S., 2022. The calcium isotope ($\delta^{44/40}$Ca) record through environmental changes: Insights from the Late Triassic. Geochemistry, Geophysics, Geosystems. 23, e2022GC010405. https://doi.org/10.1029/2022GC010405.

Kozur, H. W., 1998. Some aspects of the Permian-Triassic boundary (PTB) and of the possible causes for the biotic crisis around this boundary. Palaeogeography Palaeoclimatology Palaeoecology, 143(4), 227-272. doi:10.1016/s0031-0182(98)00113-8

Kump, L. R., Pavlov, A., & Arthur, M. A., 2005. Massive release of hydrogen sulfide to the surface ocean and atmosphere during intervals of oceanic anoxia. Geology, 33(5), 397-400. doi:10.1130/g21295.1

Lau, K. V., Maher, K., Altiner, D., Kelley, B. M., Kump, L. R., Lehrmann, D. J., Silva-Tamayo, J. C., Weaver, K. L., Yu, M., & Payne, J. L., 2016. Marine anoxia and delayed Earth system recovery after the end-Permian extinction. Proceedings of the National Academy of Sciences of the United States of America, 113(9), 2360-2365. doi:10.1073/pnas.1515080113.

Li, F., Yan, J. X., Algeo, T., & Wu, X. Z., 2013. Paleoceanographic conditions following the end-Permian mass extinction recorded by giant ooids (Moyang, South China). Global and Planetary Change, 105, 102-120. doi:10.1016/j.gloplacha.2011.09.009

Li, F., Yan, J., Chen, Z.Q., Ogg, J.G., Tian, L., Korngreen, D., Liu, K., Ma, Z., & Woods, A.D., 2015. Global oolite deposits across the Permian-Triassic boundary: a synthesis and implications for palaeoceanography immediately after the end-Permian biocrisis. Earth Sci. Rev. 149, 163–180.

Li, F., Yan, J., Burne, R. V., Chen, Z.-Q., Algeo, T. J., Zhang, W., Zhang, W., Tian, L., Gan, Y., Liu, K., & Xie, S., 2017. Paleo-seawater REE compositions and microbial signatures preserved in laminae of Lower Triassic ooids. Palaeogeography, Palaeoclima-

tology, Palaeoecology, 486, 96-107.

Li, F., Gong, Q., Burne, R. V., Tang, H., Su, C., Zeng, K., Zhang, Y., & Tan, X., 2019. Ooid factories operating under hothouse conditions in the earliest Triassic of South China. Global and Planetary Change, 172, 336-354.

Lindström, S., van de Schootbrugge, B., Dybkjær, K., Pedersen, G.K., Fiebig, J., Nielsen, L. H., Richoz, S., 2012. No causal link between terrestrial ecosystem change and methane release during the end-Triassic mass-extinction. Geology 40, 531–534.

Lindström, S., van de Schootbrugge, B., Hansen, K.H., Pedersen, G.K., Alsen, P., Thibault, N., Dybkjær, K., Bierrum, C.J., Nielsen, L.H., 2017. A new correlation of Triassic-Jurassic boundary successions in NW Europe, Nevada and Peru, and the Central Atlantic Magmatic Province: A time-line for the end-Triassic mass extinction. Palaeogeogr. Palaeoclimatol. Palaeoecol. 478, 80–102.

Lindström, S., Callegaro, S., Davies, J., Tegner, C., Van De Schootbrugge, B., Pedersen, G. K., 2021. Tracing volcanic emissions from the Central Atlantic Magmatic Province in the sedimentary record. Earth Sci. Rev. 212, 103444 https://doi.org/10.1016/j.earscirev.2020.103444.

Lucas, S. G., & Tanner, L. H., 2018. The missing mass extinction at the Triassic-Jurassic boundary. In The Late Triassic World (pp. 721-785): Springer.

Luo, G. M., Kump, L. R., Wang, Y. B., Tong, J. N., Arthur, M. A., Yang, H., Huang, J. H., Hongfu, Y., & Xie, S. C., 2010. Isotopic evidence for an anomalously low oceanic sulfate concentration following end-Permian mass extinction. Earth and planetary science letters, 300(1-2), 101-111. doi:10.1016/j.epsl.2010.09.041

Lyell, C., 1855. A manual of elementary geology: Murray.

Magaritz, M., Bart, R., Baud, A., & Holser, W. T., 1988. The carbon-isotope shift at the Permian/Triassic boundary in the Southern Alps is gradual. Nature, 331(6154), 337-339.

Marzoli, A., Renne, P. R., Piccirillo, E. M., Ernesto, M., Bellieni, G., & Min, A. D., 1999. Extensive 200-Million-Year-Old Continental Flood Basalts of the Central Atlantic Magmatic Province. Science, 284(5414), 616-618. doi:10.1126/science.284.5414.616

Marzoli, A., Callegaro, S., Dal Corso, J., Davies, J.H., Chiaradia, M., Youbi, N., Bertrand, H., Reisberg, L., Merle, R., Jourdan, F., 2018. The Central Atlantic magmatic province (CAMP): a review. In: The Late Triassic World. Springer, Cham, pp. 91–125

Maurer, F., Rettori, R., Martini, R., 2008. Triassic stratigraphy, facies and evolution of the Arabian shelf in the northern United Arab Emirates. Int. J. Earth Sci. 97 (4), 765–784.

Maurer, F., Martini, R., Rettori, R., Hillgärtner, H., Cirilli, S., 2009. The geology of Khuff outcrop analogues in the Musandam Peninsula, United Arab Emirates and Oman. GeoArabia 14 (3), 125–158.

Maxwell, W. D., 1992. Permian and Early Triassic extinction of non-marine tetrapods. Palaeontology, 35(3), 571-583.

McElwain, J.C., Beerling, D.J., & Woodward, F.I., 1999. Fossil plants and global warming at the Triassic-Jurassic boundary. Science 285 (5432), 1386–1390.

Mei, S., Henderson, C. M., & Jin, Y., 1999. Permian conodont provincialism, zonation and global correlation. Permophiles, 35(9), 16.

Newsome, L., Morris, K., & Lloyd, J. R., 2014. The biogeochemistry and bioremediation of uranium and other priority radionuclides. Chemical Geology, 363, 164-184. doi:10.1016/j.chemgeo.2013.10.034

Pálfy, J., Kovács, Z., Demény, A., Vallner, Z., 2021. End-Triassic crisis and "unreefing" led to the demise of the Dachstein carbonate platform: A revised model and evidence from the Transdanubian Range, Hungary. Global Planet. Change 199, 103428.

Paton, C., Hellstrom, J., Paul, B., Woodhead, J., & Hergt, J. (2011). Iolite: Freeware for the visualisation and processing of mass spectrometric data. Journal of Analytical Atomic Spectrometry, 26(12), 2508-2518. doi:10.1039/c1ja10172b

Payne, J. L., Lehrmann, D. J., Wei, J. Y., Orchard, M. J., Schrag, D. P., & Knoll, A. H., 2004. Large perturbations of the carbon cycle during recovery from the end-Permian extinction. Science, 305(5683), 506-509. doi:10.1126/science.1097023

Payne, J. L., Lehrmann, D. J., Follett, D., Seibel, M., Kump, L. R., Riccardi, A., Altiner, D., Sano, H., & Wei, J., 2007. Erosional truncation of uppermost Permian shallow-marine carbonates and implications for Permian-Triassic boundary events. Geological Society of America Bulletin, 119(7-8), 771-784. doi:10.1130/b26091.1

Payne, J. L., Turchyn, A. V., Paytan, A., DePaolo, D. J., Lehrmann, D. J., Yu, M. Y., & Wei, J. Y., 2010. Calcium isotope constraints on the end-Permian mass extinction. Proceedings of the National Academy of Sciences of the United States of America, 107(19), 8543-8548. doi:10.1073/pnas.0914065107

Payne, J. L., & Clapham, M. E., 2012. End-Permian mass extinction in the oceans: an ancient analog for

the twenty-first century?. Annual Review of Earth and Planetary Sciences, 40, 89-111.

Peryt, T. M., 1983. Classification of coated grains. In Coated grains (pp. 3-6): Springer.

Plee, K., Ariztegui, D., Martini, R., & Davaud, E., 2008. Unravelling the microbial role in ooid formation–results of an in situ experiment in modern freshwater Lake Geneva in Switzerland. Geobiology, 6(4), 341-350.

Posenato, R., 2008. Global correlations of mid Early Triassic events: The Induan/Olenekian boundary in the Dolomites (Italy). Earth-Science Reviews, 91(1-4), 93-105. doi:10.1016/j.earscirev.2008.09.001

Price, G. D., 1999. The evidence and implications of polar ice during the Mesozoic. Earth-Science Reviews, 48(3), 183-210. doi:10.1016/s0012-8252(99)00048-3

Racki, G., & Wignall, P. B., 2005. Late Permian double-phased mass extinction and volcanism: an oceanographic perspective. In Developments in Palaeontology and Stratigraphy (Vol. 20, pp. 263-297). Elsevier.

Rankey, E. C., & Reeder, S. L., 2009. Holocene ooids of Aitutaki Atoll, Cook Islands, South Pacific. Geology, 37(11), 971-974.

Rampino, M. R., & Caldeira, K., 2005. Major perturbation of ocean chemistry and a 'Strangelove Ocean' after the end-Permian mass extinction. Terra Nova, 17(6), 554-559. doi:10.1111/j.1365-3121.2005.00648.x

Retallack, G. J., & Jahren, A. H., 2008. Methane release from igneous intrusion of coal during Late Permian extinction events. The Journal of Geology, 116(1), 1-20.

Richoz, S., 2006. Stratigraphie et variations isotopiques du carbone dans le Permien supérieur et le Trias inférieur de quelques localités de la Néotéthys (Turquie, Oman et Iran) (pp. 1-275). Section des Sciences de la Terre, Université de Lausanne.

Richoz, S., Krystyn, L., Weidlich, O., Baud, A., Beauchamp, B., Bernecker, M., Cordey, F., Grasby, S., Henderson, C., Marcoux, J., Nicora, A., & Twitchett, R., 2010. The Permian Triassic transition in the Oman Mountains. Transect of the Tethyan margin from shallow to deep-water deposits. IGCP 572 Field Guide Book, 2.

Richoz, S., van de Schootbrugge, B., Pross, J., Püttmann, W., Quan, T. M., Lindström, S., Heunisch, C., Fiebig, J., Maquil, R., Schouten, S., Hauzenberger, C. A., & Wignall, P. B., 2012. Hydrogen sulphide poisoning of shallow seas following the end-Triassic extinction. Nature Geoscience, 5, 662. doi:10.1038/ngeo1539.

Richoz, S., Baud, A., Beauchamp, B., Grasby, S., Henderson, C., Krystyn, L., 2014. Khuff margin: slope to oceanic deposits (Permian-Triassic Allochthons and Exotics, Oman). In: Poeppelreiter,, . (Ed.), The Khuff Formation. New perspective. EAGE Publications. Houten, The Nederlands, pp. 55–76. ISBN 978-90-73834-42-2.

Riding, R., 2006. Cyanobacterial calcification, carbon dioxide concentrating mechanisms, and Proterozoic-Cambrian changes in atmospheric composition. Geobiology, 4(4), 299-316. doi:10.1111/j.1472-4669.2006.00087.x

Roduit, N., 2007. JMicroVision: un logiciel d'analyse d'images pétrographiques polyvalent. University of Geneva. Doctoral dissertation.

Roduit, N. JMicroVision: Image analysis toolbox for measuring and quantifying components of high-definition images. Version 1.3.1. https://jmicrovision.github.io (accessed 18 October 2022).

Sánchez-Beristain, F., & López-Esquivel Kranksith, L., 2011. Geochemical analyses (major, minor and trace elements, $\delta^{18}O$, and rare earths) of selected microbialites from the San Casiano Formation (Upper Triassic, NE Italy). Boletín de la Sociedad Geológica Mexicana 63 (3), 399-420.

Sandberg, P. A., 1983. An oscillating trend in Phanerozoic non-skeletal carbonate mineralogy. Nature, 305(5929), 19.

Schaltegger, U., Guex, J., Bartolini, A., Schoene, B., & Ovtcharova, M., 2008. Precise U–Pb age constraints for end-Triassic mass extinction, its correlation to volcanism and Hettangian post-extinction recovery. Earth and Planetary Science Letters, 267(1-2), 266-275.

Sepkoski, J. J., 1982. Mass extinctions in the Phanerozoic oceans: a review. Geol. Soc. Am. Spec. Pap., 190, 283-289.

Sepkoski Jr, J. J., 1990. The taxonomic structure of periodic extinction. Geological Society of America Special Paper, 247, 33-44.

Sepkoski, J.J., Jr., Bambach, R.K. & Droser, M.L., 1991. Secular changes in Phanerozoic event bedding and the biological overprint. In: Einsele, G., Ricken, W. & Seilacher, A. (eds.): Cycles and Events in Stratigraphy. Springer-Verlag, 298–312.

Sibik, S., Edmonds, M., Villemant, B., Svensen, H. H., Polozov, A. G., & Planke, S., 2021. Halogen Enrichment of Siberian Traps Magmas during Interaction with Evaporites. Front. Earth Sci. 9, 1–14.

doi:10.3389/feart.2021.741447

Siewers, F.D., 2003. Oolite and coated grains, In: Middleton, G.V., Church, M.J., Coniglio, M., Hardie, L.A., Longstaffe, F.J. (Eds.), Encyclopedia of Sedimentology. Kluwer Academic Publishers, 502-506.

Simone, L., 1980. Ooids: a review. Earth-Science Reviews, 16, 319-355.

Smith, K. S., Jakubzick, C., Whittam, T. S., & Ferry, J. G., 1999. Carbonic anhydrase is an ancient enzyme widespread in prokaryotes. Proceedings of the National Academy of Sciences of the United States of America, 96(26), 15184-15189. doi:10.1073/pnas.96.26.15184

Smrzka, D., Zwicker, J., Bach, W., Feng, D., Himmler, T., Chen, D. & Peckmann, J., 2019. The behavior of trace elements in seawater, sedimentary pore water, and their incorporation into carbonate minerals: a review. Facies, 65, Article 41. https://doi.org/10.1007/s10347-019-0581-4

Song, H. J., Wignall, P. B., Tong, J. N., & Yin, H. F., 2013. Two pulses of extinction during the Permian-Triassic crisis. Nature Geoscience, 6(1), 52-56. doi:10.1038/ngeo1649

Sorby, H. C., 1879. The structure and origin of limestones. The Popular science review, 3(9), 134-137.

Svensen, H., Planke, S., Polozov, A. G., Schmidbauer, N., Corfu, F., Podladchikov, Y. Y., & Jamtveit, B., 2009. Siberian gas venting and the end-Permian environmental crisis. Earth and planetary science letters, 277(3-4), 490-500.

Svensen, H. H., Frolov, S., Akhmanov, G. G., Polozov, A. G., Jerram, D. A.,Shiganova, O. V., Melnikov, N.V., Iyer, K., & Planke, S., 2018. Sills and Gas Generation in the Siberian Traps. Philos. Trans. R. Soc. A. 376. doi:10.1098/rsta.2017.0080

Stanley Jr, G. D., 1988. The history of early Mesozoic reef communities: a three-step process. Palaios, 170-183.

Stanley Jr, G. D., 2003. The evolution of modern corals and their early history. Earth-Science Reviews, 60(3-4), 195-225.

Stanley, S. M., 2009. Evidence from ammonoids and conodonts for multiple Early Triassic mass extinctions. Proceedings of the National Academy of Sciences of the United States of America, 106(36), 15264-15267. doi:10.1073/pnas.0907992106

Stanley Jr, G. D., & Beauvais, L., 1994. Corals from an Early Jurassic coral reef in British Columbia: refuge on an oceanic island reef. Lethaia, 27(1), 35-47.

Stanley, S.M., & Hardie, L.A., 1998. Secular oscillations in the carbonate mineralogy of reef-building and sediment-producing organisms driven by tectonically forced shifts in seawater chemistry. Palaeogeogr. Palaeoclimatol. Palaeoecol. 144, 3–19. https://doi.org/10.1016/S0031-0182(98)00109-6

Stanley, S.M., Hardie, L.A., 1999. Hypercalcification: paleontology links plate tectonics and geochemistry to sedimentology. GSA Today 9, 1–7.

Sumner, D. Y., & Grotzinger, J. P., 1993. Numerical modeling of ooid size and the problem of Neoproterozoic giant ooids. Journal of Sedimentary Research, 63(5), 974-982.

Sun, Y. D., Joachimski, M. M., Wignall, P. B., Yan, C. B., Chen, Y. L., Jiang, H. S., & Lai, X. L., 2012. Lethally hot temperatures during the Early Triassic greenhouse. Science, 338(6105), 366-370. doi:10.1126/science.1224126

Takahashi, Y., Chatellier, X., Hattori, K. H., Kato, K., & Fortin, D., 2005. Adsorption of rare earth elements onto bacterial cell walls and its implication for REE sorption onto natural microbial mats. Chemical Geology, 219(1-4), 53-67. doi:10.1016/j.chemgeo.2005.02.009

Takahashi, Y., Hirata, T., Shimizu, H., Ozaki, T., Fortin, D., 2007. A rare earth element signature of bacteria in natural waters?. Chem. Geol. 244:569–583. http://dx.doi.org/10.1016/j.chemgeo.2007.07.005.

Tan, Q., Shi, Z. J., Tian, Y. M., Wang, Y., & Wang, C. C., 2018. Origin of ooids in ooidal-muddy laminites: A case study of the lower Cambrian Qingxudong Formation in the Sichuan Basin, South China. Geological Journal, 53(5), 1716-1727

Taylor, S.R. & McLennan, S.M., 1985. The Continental Crust: Its Composition and Evolution. 312 +XV pp., Blackwell.

Tribovillard, N., Algeo, T.J., Lyons, T. & Riboulleau, A., 2006. Trace metals as paleoredox and paleoproductivity proxies: an update. Chemical Geology, 232(1-2), 12–32. https://doi.org/10.1016/j.chemgeo.2006.02.012

Trower, E.J., Cantine, M.D., Gomes, M.L., Grotzinger, J.P., Knoll, A.H., Lamb, M.P., Lingappa, U., O'Reilly, S.S., Present, T.M., Stein, N., Strauss, J.V., & Fischer, W.W., 2018. Active ooid growth driven by sediment transport in a high-energy shoal, Little Ambergris Cay, Turks and Caicos Islands. J. Sediment. Res. 88 (9), 1132–1151.

Tucker, M.E., Wilson, J.L., Crevello, P.D., Sarg, J.R., & Read, J.F. (eds), 1990. Carbonate platforms. Facies, sequences and evolution. - Spec. Publ. Int. Assoc. Sedimentologists, 9, 328 pp., Oxford (Blackwell)

Utescher, T., 1992. Mikrofazielle Untersuchungen im Unter-/Mitteldevon-Grenzbereich des westlichen Rheinischen Schiefergebirges.

Van de Schootbrugge, B., Bachan, A., Suan, G., Richoz, S., & Payne, J. L., 2013. Microbes, mud and methane: cause and consequence of recurrent Early Jurassic anoxia following the end-Triassic mass extinction. Palaeontology, 56(4), 685-709. doi:10.1111/pala.12034

Wang, Y., Sadler, P. M., Shen, S. Z., Erwin, D. H., Zhang, Y. C., Wang, X. D., Wang, W., Crowley, J. L. & Henderson, C. M., 2014. Quantifying the process and abruptness of the end-Permian mass extinction. Paleobiology, 40(1), 113-129. doi:10.1666/13022

Ward, P. D., Botha, J., Buick, R., De Kock, M. O., Erwin, D. H., Garrison, G. H., Kirschvink, J. L. & Smith, R., 2005. Abrupt and gradual extinction among Late Permian land vertebrates in the Karoo Basin, South Africa. Science, 307(5710), 709-714. doi:10.1126/science.1107068

Wei, H. Y., Shen, J., Schoepfer, S. D., Krystyn, L., Richoz, S., & Algeo, T. J., 2015. Environmental controls on marine ecosystem recovery following mass extinctions, with an example from the Early Triassic. Earth-Science Reviews, 149, 108-135. doi:10.1016/j.earscirev.2014.10.007

Wignall, P. B., & Twitchett, R. J., 1996. Oceanic anoxia and the end Permian mass extinction. Science, 272(5265), 1155-1158. doi:10.1126/science.272.5265.1155

Wilson, J.L., 1975. Carbonate facies in geologic history. 471 pp., Berlin (Springer).

Wright, V.P., 1992. A revised classification of limestones. Sed. Geol. 76 (3–4), 177–185.

Zhang, F., Romaniello, S. J., Algeo, T. J., Lau, K. V., Clapham, M. E., Richoz, S., Herrmann, A. D., Smith, H., Horacek, M., Anbar, A. D., & Anbar, A. D., 2018. Multiple episodes of extensive marine anoxia linked to global warming and continental weathering following the latest Permian mass extinction. Science advances, 4(4), e1602921.

Ziegler, M.A., 2001. Late Permian to Holocene paleofacies evolution of the Arabian Plate and its hydrocarbon occurrences. GeoArabia 6, 445–504.